Am J Cancer Res 2016;6(10):2140-2161
www.ajcr.us /ISSN:2156-6976/ajcr0033540

Original Article

Microarray expression profiling identifies genes, including cytokines, and biofunctions, as diapedesis, associated with a brain metastasis from a papillary thyroid carcinoma

Hans-Juergen Schulten[1,2], Deema Hussein[3], Fatima Al-Adwani[1,4], Sajjad Karim[1,2], Jaudah Al-Maghrabi[5,6], Mona Al-Sharif[4], Awatif Jamal[5], Sherin Bakhashab[1,7], Jolanta Weaver[7], Fahad Al-Ghamdi[5], Saleh S Baeesa[8], Mohammed Bangash[8], Adeel Chaudhary[1,2], Mohammed Al-Qahtani[1,2]

[1]Center of Excellence in Genomic Medicine Research, King Abdulaziz University, Jeddah, Saudi Arabia; [2]KACST Technology Innovation Center in Personalized Medicine, King Abdulaziz University, Jeddah, Saudi Arabia; [3]King Fahad Medical Research Center, King Abdulaziz University, Jeddah, Saudi Arabia; [4]Department of Biology, King Abdulaziz University, Jeddah, Saudi Arabia; [5]Department of Pathology, Faculty of Medicine, King Abdulaziz University Hospital, Jeddah, Saudi Arabia; [6]Department of Pathology, King Faisal Specialist Hospital and Research Center, Jeddah, Saudi Arabia; [7]Institute of Cellular Medicine, Newcastle University, Newcastle NE2 4HH, United Kingdom; [8]Division of Neurosurgery, Department of Surgery, King Abdulaziz University Hospital, Jeddah, Saudi Arabia

Received September 21, 2016; Accepted September 23, 2016; Epub October 1, 2016; Published October 15, 2016

Abstract: Brain metastatic papillary thyroid carcinomas (PTCs) are afflicted with unfavorable prognosis; however, the underlying molecular genetics of these rare metastases are virtually unknown. In this study, we compared whole transcript microarray expression profiles of a *BRAF* mutant, brain metastasis from a PTC, including its technical replicate (TR), with eight non-brain metastatic PTCs and eight primary brain tumors. The top 95 probe sets (false discovery rate (FDR) *p*-value < 0.05 and fold change (FC) > 2) that were differentially expressed between the brain metastatic PTC, including the TR, and both, non-brain metastatic PTCs and primary brain tumors were in the vast majority upregulated and comprise, e.g. *ROS1*, *MYBPH*, *SLC18A3*, *HP*, *SAA2-SAA4*, *CP*, *CCL20*, *GFAP*, *RNU1-120P*, *DMBT1*, *XDH*, *CXCL1*, *PI3*, and *NAPSA*. Cytokines were represented by 10 members in the top 95 probe sets. Pathway and network analysis (*p*-value < 0.05 and FC > 2) identified granulocytes adhesion and diapedesis as top canonical pathway. Most significant upstream regulators were lipopolysaccharide, TNF, NKkB (complex), IL1A, and CSF2. Top networks categorized under diseases & functions were entitled migration of cells, cell movement, cell survival, apoptosis, and proliferation of cells. Probe sets that were significantly shared between the brain metastatic PTC, the TR, and primary brain tumors include *CASP1*, *CASP4, C1R*, *CC2D2B, RNY1P16*, *WDR72*, *LRRC2*, *ZHX2*, *CITED1,* and the noncoding transcript AK128523. Taken together, this study identified a set of candidate genes and biofunctions implicated in, so far nearly uncharacterized, molecular processes of a brain metastasis from a PTC.

Keywords: Papillary thyroid carcinoma, brain metastasis, microarray expression profiling, cytokines, diapedesis

Introduction

Approximately 80% of all thyroid carcinomas are histologically classified as papillary thyroid carcinomas (PTCs). PTCs harbor in 40-70% of the cases a *BRAF* V600E mutation that renders BRAF in a constitutively active formation and has shown to confer vulnerability to protease inhibitors [1]. In thyroid cancer, the V600E mutation is frequently associated with unfavorable features including multifocality, lymph node involvement, and distant metastasis. We reported earlier on the comparison between V600E positive and negative PTCs and normal thyroid samples, revealing that V600E positive PTCs are comparably afflicted with more unfavorable features; however, both V600E positive and negative PTCs exhibited quite closely related expression profiles when compared to normal thyroid samples [2].

Common sites of distant PTC metastases are lung and bone whereas metastases to the brain are rare. Frequency of brain metastases varies between 0.15-1.3% of all diagnosed thyroid carcinomas [3]. Brain metastases can occur even after years of the primary thyroid tumor with an approximately 10 years difference of patients' mean age; however, aggressive subtypes of PTC as tall cell variants are likely to metastasize earlier than other histological subtypes [4]. Prognosis for patients with intracranial brain metastasis of a PTC is in general poor and depends on factors like histology type and the presence of other distant metastases [5]. In approximately 10% of patients who die from thyroid carcinoma reveal to have a brain metastasis at autopsy [6].

Symptoms implicative for a brain metastasis include headache, nausea, seizure, polyuria, and various neuronal impairments such as ocular motor vision dysfunction. Asymptotic brain metastases from thyroid cancer are very rare and can be incidentally detected by ^{131}I treatment. Treatment options include surgery, radiation, and systemic therapy. Surgical resection of a brain metastasis originating from differentiated thyroid cancer may improve prognosis of patients [6]. Sorafenib which is a dual-active inhibitor that inhibits the mitogen activated protein kinase pathway has been successfully applied to treat a patient with a brain metastasis originating from a follicular thyroid carcinoma [7]. It is proposed that the brain metastatic process is a multistep process involving migration, intravasation, circulation, arrest, extravasation, and settlement/invasion of the brain microenvironment [8, 9].

In the present study, using whole transcript microarrays, we analyzed the expression profile of a brain metastasis from a PTC and compared it with those from non-brain metastatic, stage III and IV PTCs and with primary brain tumors. Our objectives were to identify molecular biomarkers that are specifically related to the brain metastatic PTC and that support unraveling molecular mechanisms underlying this deteriorative disease.

Material and methods

Tumor samples

In the core expression analysis we studied samples from one brain metastatic PTC, eight non-brain metastatic, stage III and IV PTCs and eight primary brain tumors. The specimens were derived from patients who were treated surgically in the period between 2010 and 2015 at the King Abdulaziz University Hospital, Jeddah, and the King Faisal Specialist Hospital and Research Center (KFSH&RC), Jeddah. Histopathological diagnosis was performed by a team of pathologists (JM, AJ, and FG) on established criteria. The brain metastasis was initially identified as a left frontal brain tumor in a middle-aged (< 45 years) old female without any known chronic illness and the tumor was treated by surgery. Histopathological examination sustained the diagnosis of a metastatic PTC and subsequent sonography demonstrated thyroid nodules and the primary, stage II [10], multifocal PTC and lymph node metastases were resected. This study was approved by the Research Ethics Committee of the King Abdulaziz University, Faculty of Medicine, #358-10, #976-12, and the Institutional Review Board of the KFSH&RC, #IRB2010-07.

Immunohistochemistry

Antibodies (Ventana Medical Systems, Tucson, AZ) employed for immunohistochemistry (IHC) consisted of thyroid transcription factor (TTF-1) (clone 8G7G3/1), thyroglobulin (clone 2H11/6E1), and proliferation marker ki-67 (clone 30-9) which is immunoreactive in the late G1, S, G2, and M phases of the cell cycle. Four µm sections of formalin-fixed and paraffin-embedded specimens were processed on an automated immunostainer (BenchMark XT, Ventana Medical Systems) according to the manufacturer's protocols and using the ultraView Universal DAB Detection Kit for detection.

RNA and microarray processing

Isolation of total RNA and microarray sample processing were performed as described earlier [14, 15]. In brief, the Agilent 2100 Bioanalyzer (Agilent Technologies, Palo Alto, CA) was employed to assess RNA integrity and integrity number was > 5 in samples used for the differential expression analysis between then brain metastatic PTC, non-brain metastatic PTCs, and primary brain tumors. The NanoDrop ND-1000 spectrophotometer (NanoDrop Technologies, Wilmington, DE) was utilized to determine RNA concentration. All RNA samples were processed using the Ambion WT Expression Kit (Life Technologies, Austin, TX), the GeneChip

WT Terminal Labeling and Controls Kit (Affymetrix, Santa Clara, CA), and the Affymetrix GeneChip Hybridization, Wash and Stain Kit. The RNA from the brain metastasis was processed twice to generate a technical replicate (TR). All processed samples were hybridized to Affymetrix Human Gene 1.0 ST GeneChip arrays. This type of microarray interrogates with a set of 764,885 probes 36.079 annotated reference sequences (NCBI build 36). The microarrays were scanned on a GeneChip Scanner 3000 7G and probe cell intensity data (CEL) files were generated using the GeneChip Command Console Software (AGCC).

Sample selection for microarray expression study

Sample selection criterion was to identify probe sets which are significant to the brain metastatic process. Therefore, eight non-brain metastatic, stage III and IV PTCs as advanced thyroid tumors and eight selected primary brain tumors were chosen for differential expression analysis. For selection, analysis of variance (ANOVA) in Partek Genomics Suite version 6.6 (Partek Inc., MO) was employed and performed on the imported CEL files and carried out between the comparison group, consisting of the brain metastatic PTC and its TR, and each of 40 primary brain tumors for which CEL files were available from our microarray data sets. Eight primary brain tumors with meningioma histology revealed to have the comparably lowest numbers of differentially expressed probe sets with the brain metastatic PTC and its TR (p-value < 0.05 and FC > 2) and therefore were taken, after assessing sample bias, as a group for differential gene expression analysis which included also, besides the brain metastatic PTC and its TR, the eight non-brain metastatic PTC group. Sample bias was assessed by replacing the eight primary brain tumors with comparably lowest numbers of differentially expressed probe sets with those eight brain tumors having the highest number of differentially expressed probe sets. The ANOVA result of the assessment showed that approximately 90% of the significantly differentially expressed probe sets were shared between both configurations.

Gene expression core analysis

In Partek Genomics Suite quality assessment of microarray experiments was performed on basis of QC metrics tables and QC graphical reports on the imported CEL files. The saved distribution file of 18 quantile normalized samples was used for quantile normalization of subsets of the 18 CEL files, i.e. 17 CEL files consisting of eight non-brain metastatic PTCs, eight primary brain tumors and either the brain metastatic PTC or its TR. All lists of differentially expressed probe sets were generated by applying ANOVA and using either a p-value < 0.05 and a fold change (FC) > 2 or using, where indicated, the more stringent criterion of the false discovery rate (FDR) p-value (step-up method) < 0.05, and fold change (FC) > 2. Principal component analysis was employed to illustrate overall variance in gene expression between samples or groups of samples. Average linkage hierarchical clustering was performed by using Spearman's correlation as a similarity matrix. Venn diagrams were generated to display intersecting or non-intersecting groups of differentially expressed probe sets. The Gene Ontology (GO) enrichment tool was employed in the gene expression workflow to group significantly expressed genes into functional categories. The gene enrichment score utilizes the Fisher's Exact test to determine the level of differential gene expression in a functional category. PANTHER version 10 which combines GO annotations and a phylogenetic tree model for inferring gene functions was primarily used for protein classification [16]. The generated microarray data set has been deposited at the NCBI Gene Expression Omnibus under accession number GSE66463 and it includes renormalized samples from non-brain metastatic PTCs and primary brain tumors of submissions GSE54958 [2, 17] and GSE77259 [11].

Functional network and pathway analysis

The Ingenuity Pathways Analysis software (IPA; build version 338830M) (Ingenuity Systems, Redwood City, CA) was utilized to interpret biological significance of expression data [18]. IPA workflow comprises core and functional analysis and structural data categorization. The Ingenuity Knowledge Base was used as a reference data set. Direct and indirect molecular relationships were included in the analysis settings. Fisher's exact test p-values indicate the significance of relationships between the analyzed data set molecules and the functional frameworks prebuilt or generated *de novo* by IPA. Where specified, the Molecule Activity

Table 1. Primer sequences used for semiquantitative RT-PCR

Gene	Forward primer sequence (5'-3')	Reverse primer sequence (5'-3')	Product size (bp)
ROS1	ATTGTGGAGAGTTGCACG	ATGACCTTGCCATCTGTG	205
MYBPH	CCAGTCCAGCAATGATGG	AGGCTTAGTGGCTGTGGA	202
SLC18A3	GCGAAGACGTGAAGATCG	ATGGCTATGCCAGACGTG	240
HP	CTACACCCTAACTACTCC	ACATACTTCAGATGGTCAGT	184
CP	ACCCTGATAACACCACAG	AAGGTCCGATGAGTCCTG	185
CCL20	ACCATGTGCTGTACCAAG	ATGTCACAGCCTTCATTGG	178
GFAP	GCTTTGCCAGCTACATCG	ATTGTCCCTCTCAACCTC	193
SAA2	TTTTCGTTCCTTGGCGAG	CTCTCTACAGTTCAGCTG	192

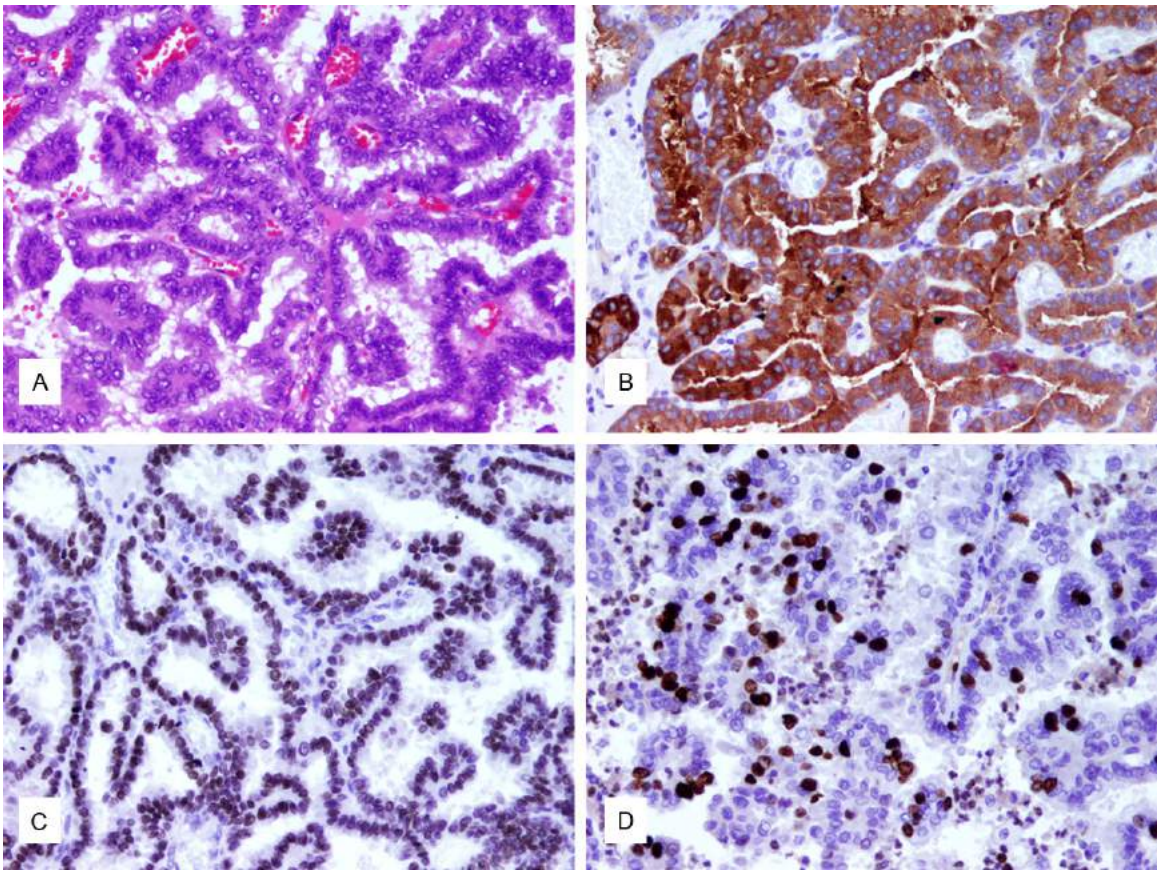

Figure 1. The brain metastatic PTC. A. Hematoxylin-eosin staining reveals papillary architectures covered by cuboidal to columnar epithelium. Cellular crowding is visible and neoplastic cells demonstrate nuclear clearing and nuclear grooves. B. TTF-1 staining as a marker for thyroid or lung origin exhibits strong nuclear staining. C. Thyroglobulin shows strong cytoplasmic staining. D. Proliferation marker Ki67 is positive in 20% of cells (original magnification, x400).

Predictor was utilized to predict expression effects/coherence of expression effects of a molecule on other pathway or network molecules. The canonical pathway workflow was employed to identify molecules from the uploaded data set that are co-expressed in a directional, up- to downstream, pathway. The overlap percentage of uploaded molecules matching to a canonical pathway determines its overrepresentation and ranking. Upstream regulators analysis was employed to explain how differences in target gene expression are regulated by upstream molecules and what kind of biological activities are involved. The activation z-score predicts the activation states of regulators. The diseases & functions net-

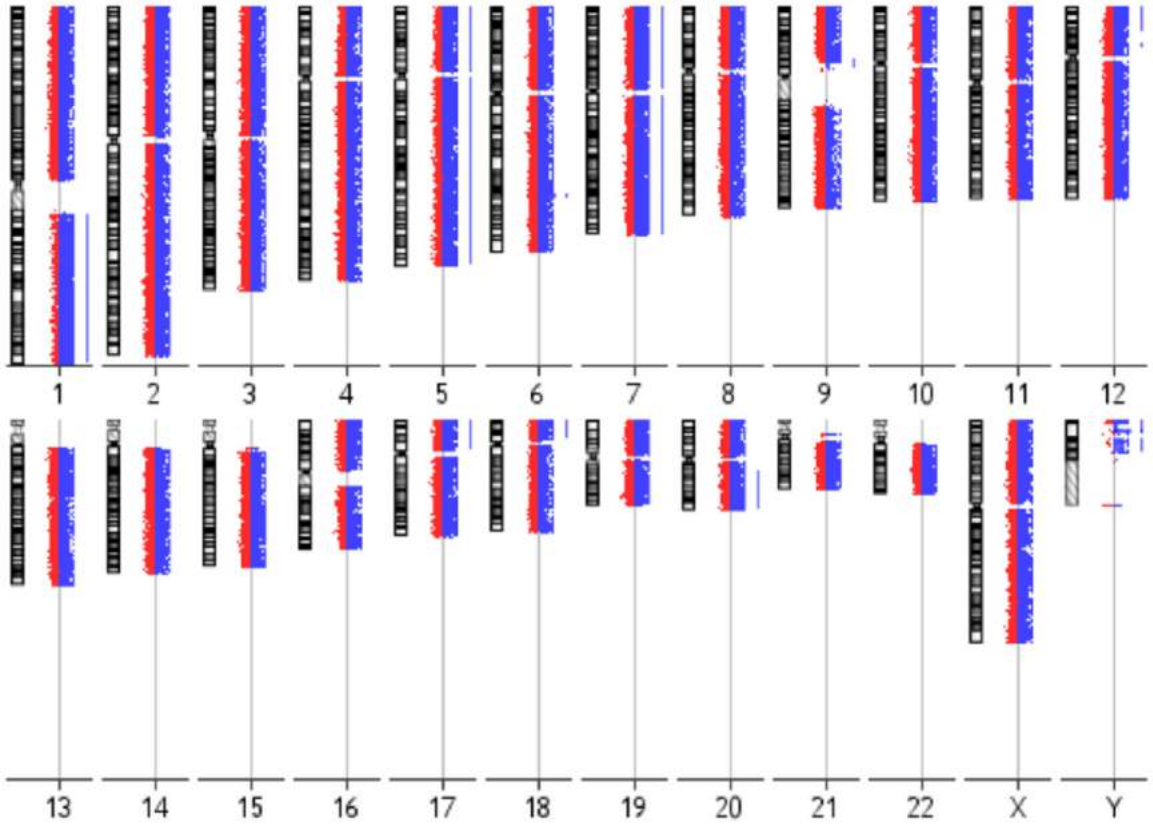

Figure 2. aCGH karyogram of the brain metastatic PTC. Each chromosome ideogram is shown with the green/red fluorescent profiles representing oligonucleotide features. Bars to the right of the profiles indicate gains affecting chromosomes/chromosomal regions including 1q, 5, 7, 12p12pter, 17p, 18p, and 20q.

work analysis was employed to explore relationships and effects between the uploaded data set and downstream processes. The activation z-score measures in how far downstream processes are either up- or downregulated.

Semiquantitative RT-PCR and BRAF mutational analysis

Expression of eight genes was assessed by semiquantitative RT-PCR using housekeeping gene *B2M* as reference. Primer sequences of the genes are listed in **Table 1** and in case of *B2M* have been reported previously [11]. RT-PCR were performed in 20 µL volumes containing each 2 µL buffer mix, 0.1% 2-mercaptoethanol, 0.0125% BSA, 3 mM $MgCl_2$, 10 nmol of each dNTP, 5 pmol forward primers, 5 pmol reverse primers, 1.25 units GoTaq DNA Polymerase (Promega, Madison, WI), and 200 ng of second strand cDNA template that was generated using the Ambion WT Expression Kit. No cDNA template was included in the negative control. A modified standard PCR protocol was used as reported earlier [11]. Gel band densities of selected reactions were measured using ImageJ 1.49v [12] and then the ratio to the internal reference *B2M* was calculated. DNA extraction and *BRAF* mutational screening for the non-brain metastatic PTCs was reported earlier (GSE54958) and for the brain metastatic PTC was performed within the present study as described by us [13].

aCGH analysis

aCGH study of the brain metastatic PTC was performed according to the manufacturer's protocol (Agilent Technologies, Santa Clara, CA). In brief, tumor DNA was extracted by using the QIAmp DNA FFPE tissue kit (Qiagen, Hilden, Germany). Subsequently, 500 ng of tumor DNA and 500 ng fragmented Agilent, gender-matched reference DNA were labeled using ULS-Cy3 and ULS-Cy5 reagents (Genomic DNA ULS labeling kit), respectively. The hybridization mixture, containing 5 µg human Cot-1 DNA, 1 µL 100x blocking reagent, 2x Hi-RPM hybridization

Table 2. Demographic data and clinicopathological tumor features

Case	Histology[1]	Age	Gender[2]	Tumor location[3]	Tumor stage
TM-1039-11	Conventional PTC	52	F	Jugular vein wall	IV
TM-989-11	FVPTC	71	F	Skull, bone	IV
TM-602-11	Conventional PTC	59	F	Thyroid bed, lung	IV
TM-187-11	Conventional PTC	56	M	Lymph node, perithyroidal extension	IV
TM-892-11	Conventional PTC	56	M	Thyroid bed	IV
TM-279-08	Conventional PTC	77	M	Cervical and retropharyngeal lymph nodes	III
TM-301-12	FVPTC	51	F	No recurrence/metastasis	III
TM-824-12	Conventional PTC	55	F	Extrathyroidal extension	IV
Jed51_MTT	Conventional PTC	44	F	Brain, left frontal	II
Jed04_MN	Transitional meningioma	57	F	Left tentoral	I
Jed13_MN	Meningothelial meningioma	50	F	Left frontal	I
Jed49_MN	Atypical meningioma with brain invasion	51	F	Posterior right subfalcine	II
Jed57_MN	Transitional meningioma	48	F	Left parasagittal	I
Jed64_MN	Fibroblastic meningioma	49	F	Right frontal	I
Jed70_MN	Fibroblastic meningioma	73	F	Right temporal	I
Jed88_MN	Secretory meningioma	43	M	Sub-occipital	I
Jed92_MN	Meningothelial meningioma	49	F	Olfactory groove	I

[1]FVPTC, follicular variant of PTC; [2]F, female, M, male; [3]Tumor location, location of PTC recurrence/metastasis and location of primary brain tumors including one recurrence (Jed49_MN).

buffer, and both labeled DNA solutions was hybridized for 40 hrs at 65°C and 20 rpm to a 180K SurePrint G3 Human CGH microarray. The type of microarray contains 170,334 distinct biological features. Subsequently, the microarray was washed stringently, then scanned using the SureScan High resolution scanner, and the generated TIFF image analyzed, utilizing CytoGenomics v3.0.6 software (Agilent Technologies) according to its user guide (G1662-90046). Confidence of differential expression of biological features is based on *p*-values that are generated using the log ratios of the Cy3 to Cy5 channel signals and the log ratio errors which are a measure for the significance of computed log ratios.

Results

Hematoxylin-eosin staining revealed a characteristic papillary architecture of the brain metastatic PTC (**Figure 1A**). Nuclear immunoreactivity for TTF-1 and cytoplasmic immunoreactivity for thyroglobulin demonstrated origin of the brain metastasis from a PTC (**Figure 1B**, **1C**). Proliferation marker Ki-67 showed immunoreactivity in about 20% of the tumor cells (**Figure 1D**). Five of the non-brain metastatic PTCs and the brain metastatic PTC exhibited a *BRAF* V600E mutation. An aCGH analysis of the brain metastasis identified a number of whole and partial chromosomal gains including +1q, +5, +7, +12p12pter, +17p, +18p, and +20q (**Figure 2**).

Genes differentially expressed in the brain metastasis and the TR vs. non-brain metastatic PTCs and primary brain tumors

A detailed microarray expression analysis was performed on a rare brain metastasis from a PTC, including its TR, eight non-brain metastatic, stage III and IV PTCs and eight primary brain tumors (**Table 2**). The primary brain tumors were of meningioma histology and selected as described under Material and methods. Similarity of expression profiles of all 18 samples is illustrated by a distance related scale in a PCA 3D scatter plot (**Figure 3**). Hierarchical cluster analysis separately groups the brain metastatic PTC and the TR, from non-brain metastatic PTCs, and primary brain tumors (**Figure 4**). The 18 tumor samples served as basis to generate four differentially expressed comparison groups, i.e. brain metastatic PTC *vs*. non-brain metastatic PTCs, brain metastatic PTC (TR) *vs*. non-brain metastatic PTCs, brain metastatic PTC *vs*. primary brain tumors, and brain metastatic PTC (TR) *vs*. primary brain tumors. The top 95 differentially expressed probe sets, that

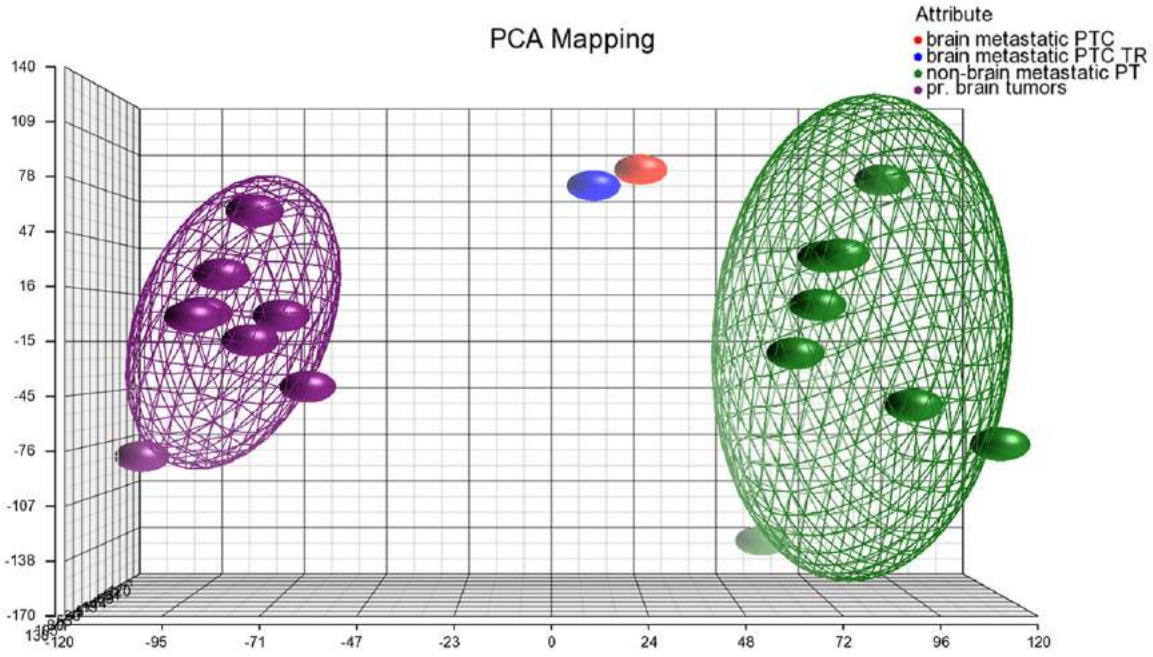

Figure 3. PCA 3D scatter plot as a dimensional, distance-related measure to display similarity of expression profiles of samples that are indicated by dots. Bounding ellipsoids are included for non-brain metastatic PTCs and primary brain tumors. Colors for samples/groups of samples as indicated in the color scheme legend.

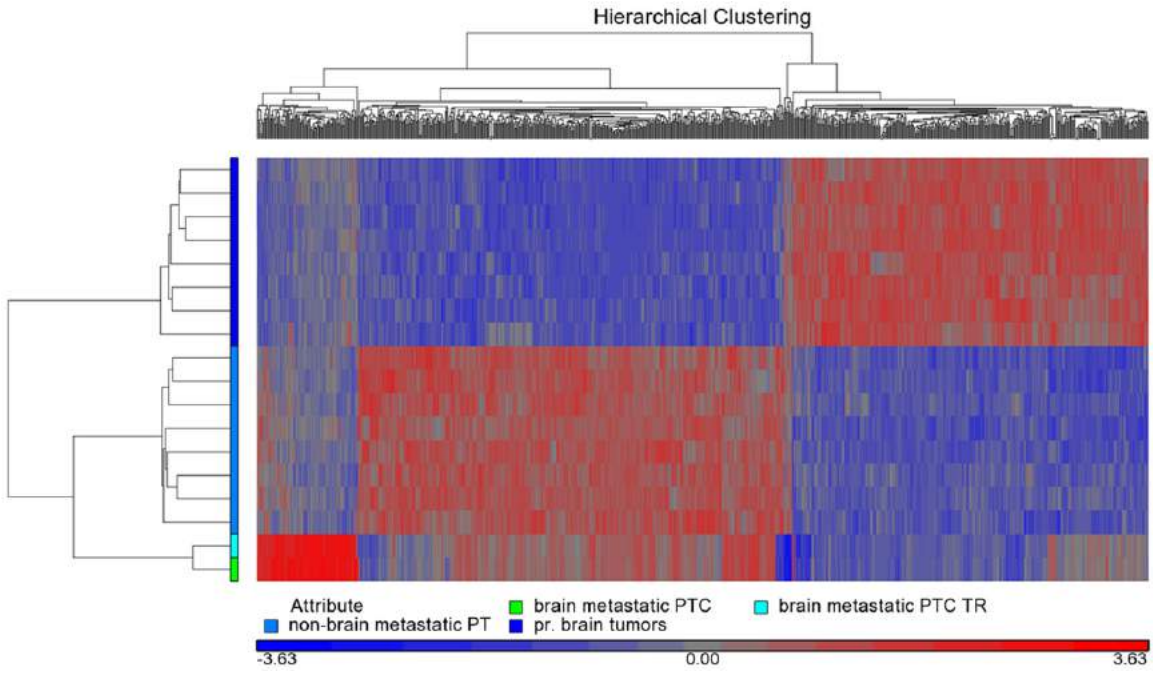

Figure 4. Hierarchical cluster analysis between the brain metastatic PTC, the TR, non-brain metastatic PTCs, and primary brain tumors. The brain metastatic PTC and the TR are clustering separately from the two other groups. Analysis is based on 796 differentially expressed probe sets (p-value < 0.0005). Colors for samples/groups of samples as indicated in the color scheme legend.

primarily distinguish the brain metastatic PTC from both, non-brain metastatic PTCs and primary brain tumors were those that intersect with all four comparison groups (**Figure 5A**,

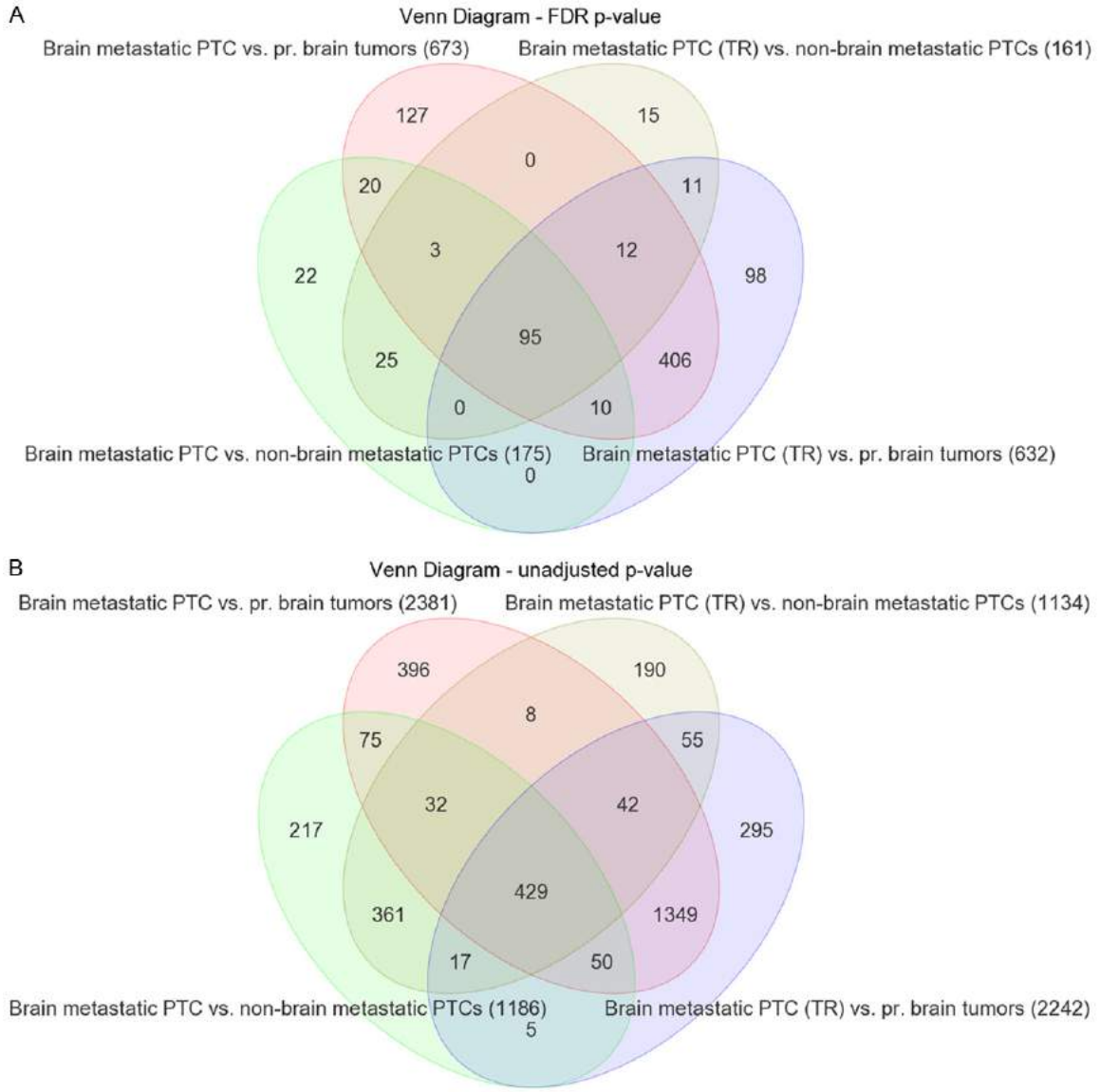

Figure 5. Venn diagrams displaying differentially expressed probe sets that intersect or non-intersect between different comparison groups. A. Applying a FDR *p*-value < 0.05 and FC > 2.0 results in 95 differentially expressed probe sets (Supplement Table 1) that intersect between the four comparison groups brain metastatic PTC *vs*. non-brain metastatic PTCs, brain metastatic PTC (TR) *vs*. non-brain metastatic PTCs, brain metastatic PTC *vs*. primary brain tumors, and brain metastatic PTC (TR) *vs*. primary brain tumors. The 95 probe sets include 90 genes represented by one probe set each, 2 genes represented by two probe sets each, and one unmapped transcript. B. Applying the unadjusted *p*-value < 0.05 and FC > 2.0 results in 429 differentially expressed probe sets that intersect between the comparison groups as outlined under A (Supplement Table 1). Numbers of probe sets that are differentially expressed in each comparison group are given in parentheses.

Supplement Table 1). The 95 probe sets were in the vast majority comparably upregulated in the brain metastatic PTC. The encoded proteins/molecules represent various functional categories. These include the cytokines CCL20, CXCL1, CCL13, OSM, CXCL8, IL6, IL17C, CXCL2, IL1B, and IL32; proteins with receptor activity, e.g. ROS1, FPR2, IL1R2, and SIGLEC6; cytoskeletal and related proteins, e.g. MYBPH, GFAP, KRT17, ACTBL2, and TUBB3; enzymes including proteases and their inhibitors, e.g. XDH, PI3, NAPSA, FSTL5, SPINK14, TMPRSS3, and MMP7; and transporter proteins, e.g. SLC18A3, CP, CNTNAP5, AQP5, and SLC6A14. Molecules of various categories were, e.g. HP, SAA1, SAA2, SAA2-SAA4, DMBT1, ZER1,

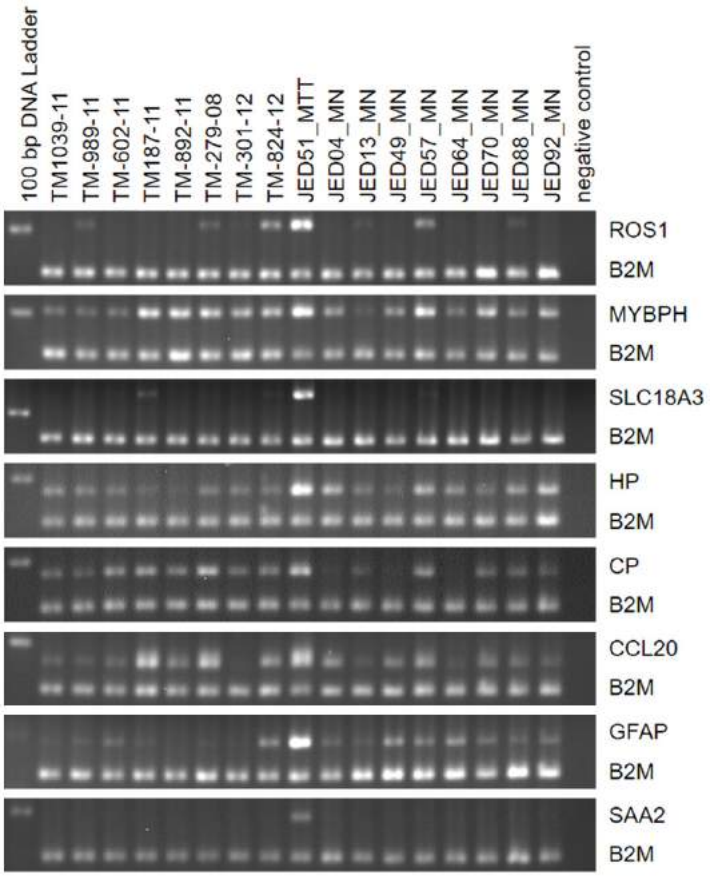

Figure 6. Semiquantitative RT-PCR for *ROS1, MYBPH, SLC18A3, HP, CP, CCL20, GFAP,* and *SAA2* in the case series of eight thyroid tumors (TM-1039-11, TM-989-11, TM-602-11, TM-187-11, TM-892-11, TM-279-08, TM-301-12, and TM-824-12), the brain metastatic thyroid tumor (Jed51_MTT) and eight primary brain tumors (Jed04_MN, Jed13_MN, Jed49_MN, Jed57_MN, Jed64_MN, Jed70_MN, Jed88_MN, and Jed92_MN). The genes rank among the top differentially expressed probe sets (Supplement Table 1). The PCR products of the interrogated genes have a size between 178-240 bp (**Table 1**). Product size of the internal reference gene *B2M* is 156 bp. Relative band densities of the PCR products for all eight genes compared to *B2M* is comparably highest for Jed51_MTT. Some cases as e.g. Jed57_MN express considerable amounts of *MYBPH* (~55%, compared to Jed51_MTT), or TM-279-08 express considerable amounts of *CP* (~69%) and *CCL20* (~64%). Lane 1 contains the DNA ladder with the 200 bp band visible in the image fields and lane 19 contains the negative control reactions.

HSPA6, OTX2, RRAD, RAB7B, MIR146A, SBSN, and FAM83A. Eight differentially expressed genes, i.e. *ROS1*, *MYBPH*, *SLC18A3*, *HP*, *CP*, *CCL20*, and *GFAP* were subjected to semiquantitative RT-PCR that substantially confirmed microarray expression data (**Figure 6**).

Biofunctional prediction analysis

Biofunctional analysis was performed on the set of 429 differentially expressed probe sets (p-value < 0.05 and FC > 2) (**Figure 5B**, Supplement Table 1). Functional groups that were significantly over-represented in different ontology categories are illustrated in a GO enrichment analysis (**Figure 7**). In the cellular component domain, the categories extracellular region part, extracellular region, and membrane-enclosed lumen were prevalent. In the molecular function domain, the most significantly related categories were molecular transducer activity, antioxidant activity, and chemoattractant activity. In the biological process domain, the prevalent categories were locomotion, single-organism process, and response to stimuli. The top canonical pathway was entitled granulocyte adhesion and diapedesis, illustrating molecular processes implicated in transendothelial migration (**Table 3**, **Figure 8**). Other top pathways were likewise related to inflammatory response and diseases. Network analysis identified as most significantly related upstream regulators lipopolysaccharide, the nuclear NFkB (complex), and the cytokines TNF, Il1A, and CSF2, otherwise known as GM-CSF (**Table 3**, **Figure 9**). Top networks under the category diseases & functions were entitled migration of cells, cell movement, cell survival, apoptosis, and proliferation of cells (**Table 3**, **Figure 10**).

Genes shared between the brain metastasis and primary brain tumors

To identify candidate genes that may support the brain metastasis to adapt and expand in the brain microenvironment, we selected (FDR p-value < 0.05 and FC > 2.0) in our data set for those probe sets that intersect between the comparison groups, brain metastatic PTC *vs*. non-brain metastatic PTCs, brain metastatic PTC (TR) *vs*. non-brain metastatic PTCs, and primary brain tumors *vs*. non-brain metastatic PTCs. Furthermore, we excluded from the intersecting probe sets those that were included in the list of 429 probe sets. The resulting probe

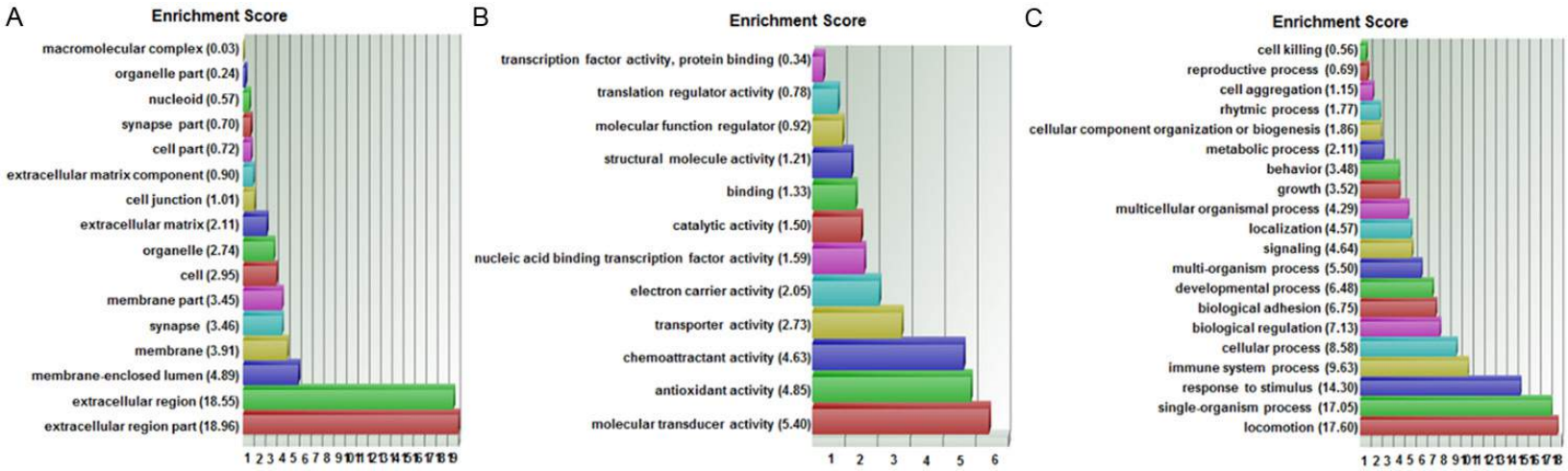

Figure 7. GO enrichment analysis for the 429 differentially expressed probe sets. The functional categories are ranked according to their *p*-values. A. The categories extracellular region part, extracellular region, and membrane-enclosed lumen were most overrepresented in the cellular component domain. B. The most over-represented categories in the molecular function domain were molecular transducer activity, antioxidant activity, and chemoattractant activity. C. The dominant categories in the biological process domain were locomotion, single-organism process, and response to stimulus.

Table 3. Top pathways and networks based on 429 differentially expressed probe sets

Category	Brain metastatic PTC *vs*. non-brain metastatic PTCs		Brain metastastic PTC *vs*. primary brain tumors	
	p-value	Overlap [%]/activation z-score	*p*-value	Overlap [%]/activation z-score
Top canonical pathways				
Granulocyte adhesion and diapedesis	1.38E-09	11.4	1.38E-09	11.4
Agranulocyte adhesion and diapedesis	8.24E-07	8.9	8.24E-07	8.9
Role of IL-17A in psoriasis	2.79E-06	38.5	2.79E-06	38.5
LXR/RXR activation	3.21E-06	10.0	3.21E-06	10.0
Acute phase response signaling	4.04E-06	8.4	4.04E-06	8.4
Top upstream regulators				
Lipopolysaccharide	1.81E-23	6.382	1.81E-23	6.734
TNF	2.82E-23	5.799	2.82E-23	6.102
NFkB (complex)	2.99E-22	5.477	2.99E-22	5.477
IL1A	4.46E-20	4.668	4.46E-20	5.016
CSF2	4.12E-18	4.729	4.12E-18	4.729
Diseases & functions				
Migration of cells	9.77E-14	5.694	9.77E-14	4.989
Cell movement	1.48E-13	5.982	1.48E-13	5.298
Cell survival	3.24E-13	5.493	3.24E-13	5.203
Apoptosis	6.63E-13	-0.923	6.63E-13	-2.397
Proliferation of cells	1.22E-12	4.191	1.22E-12	4.063

sets include *CASP1*, *CASP4*, and *C1R* which were comparably higher expressed and *CC2-D2B, RNY1P16*, *WDR72*, *LRRC2*, *ZHX2*, *CITED1,* and the noncoding and uncharacterized transcript AK128523 which were comparably lower expressed in the brain metastatic PTC.

Discussion

In contrast to melanoma, breast and lung cancer, which contribute to the majority of cancers with brain metastasis, brain metastatic PTCs are rare and presence of a PTC brain metastasis prior to detection of the primary thyroid tumor is exceptionally rare [19]. We present to our knowledge the first whole transcript expression profile of a brain metastasis from a PTC. Critical steps of the brain metastatic process as transmigration through the blood brain barrier (BBB) are not fully explored yet and depend on a number of factors as tissue type of tumor cells, cellular interactions and the time interval needed for extravasation [8, 9]. By comparing the expression profile of a brain metastasis with profiles of advanced stage, non-brain metastatic PTCs and with profiles of statistically sorted primary brain tumors, we selected for those differentially expressed candidate genes that are most probably related to *in vivo* characteristics of the brain metastatic process. The *BRAF* mutational status of PTC metastases to the brain has only been reported for a small number of cases providing limited information to the clinical behavior of these metastases [20, 21]. A meta-analysis revealed that distant metastases from PTCs are not significantly associated with the *BRAF* mutational status [22]; however, a positive *BRAF* mutational status was more frequently observed in PTCs with a brain metastasis in comparison to other metastatic sites as soft tissue, lung, and retroperitoneum [20].

Cytokines

CCL20 is a ligand for CCR6 and its expression is a proinflammatory signal, known to be upregulated in a number of cancer types. In SW1736 thyroid cancer cells, migration and invasion was induced by activation of CCR6 through CCL20 [23]. In addition, CCL20 stimulated expression and secretion of MMP3 and the nuclear translocation and activation of NFkB which is known to be implicated in a variety of cellular functions including cytokine activation and exertion of pro-tumorigenic activities. Of notice,

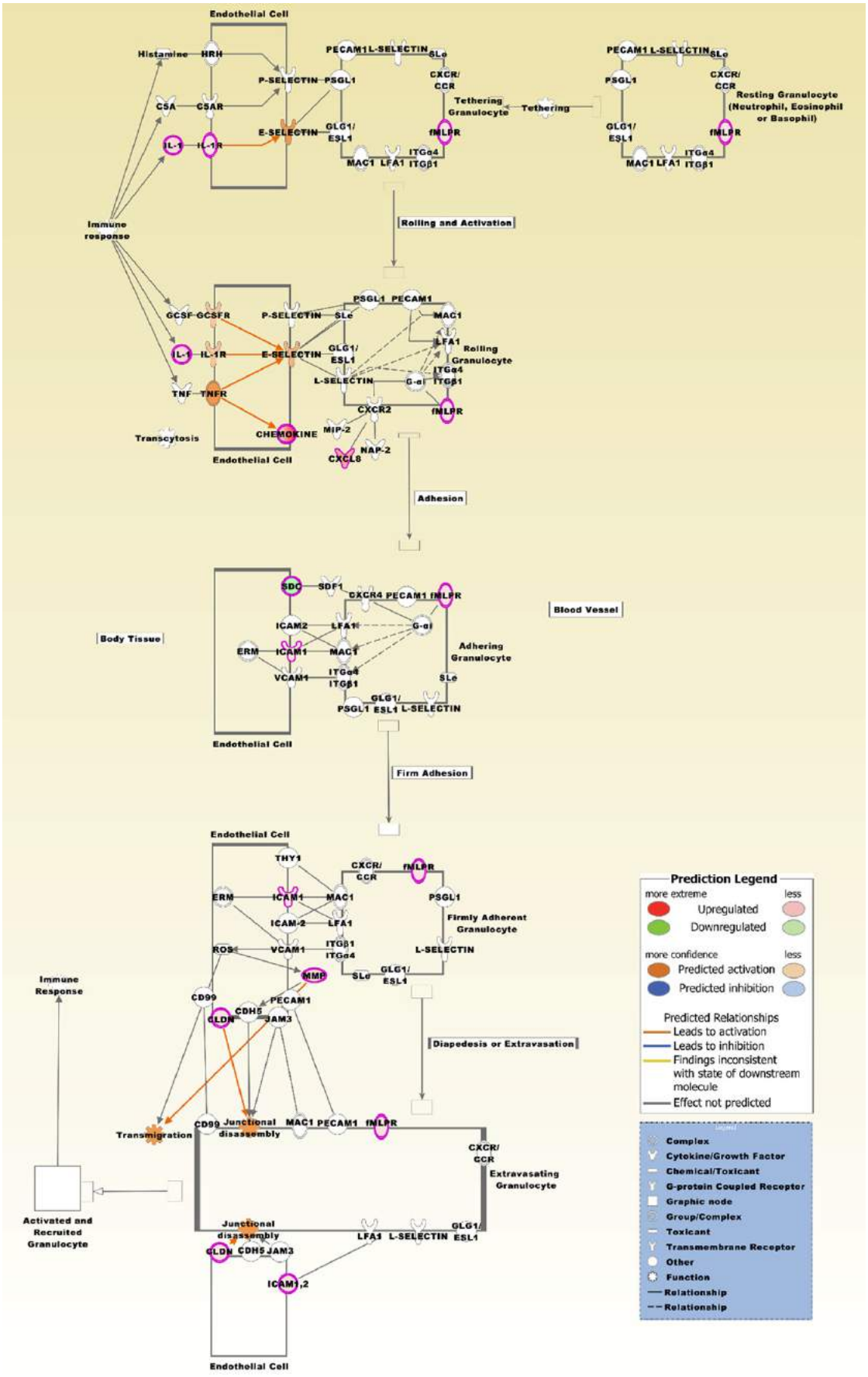
Endothelial Cell
Histamine
HRH
P-SELECTIN
PSGL1
PECAM1
L-SELECTIN
SLe
CXCR/
CCR
C5A
C5AR
Tethering
Granulocyte
Tethering
Resting Granulocyte
(Neutrophil, Eosinophil
or Basophil)
E-SELECTIN
GLG1/
ESL1
fMLPR
IL-1
IL-1R
MAC1
LFA1
ITGα4
ITGβ1
Immune
response
Rolling and Activation
GCSF
GCSFR
Rolling
Granulocyte
G-αi
TNF
TNFR
CXCR2
Transcytosis
CHEMOKINE
MIP-2
NAP-2
CXCL8
Adhesion
Blood Vessel
Body Tissue
SDC
SDF1
CXCR4
ICAM2
ICAM1
ERM
VCAM1
Adhering
Granulocyte
Firm Adhesion
THY1
ROS
MMP
Firmly Adherent
Granulocyte
Immune
Response
CD99
CDH5
CLDN
JAM3
Diapedesis or Extravasation
Transmigration
Junctional
disassembly
Extravasating
Granulocyte
Activated and
Recruited
Granulocyte
ICAM1,2
Prediction Legend
more extreme
less
Upregulated
Downregulated
more confidence
Predicted activation
Predicted inhibition
Predicted Relationships
Leads to activation
Leads to inhibition
Findings inconsistent
with state of downstream
molecule
Effect not predicted
Complex
Cytokine/Growth Factor
Chemical/Toxicant
G-protein Coupled Receptor
Graphic node
Group/Complex
Toxicant
Transmembrane Receptor
Other
Function
Relationship
Relationship

Figure 8. The top canonical pathway is entitled granulocyte adhesion and diapedesis. The pathway is based on the list of 429 differentially expressed probe sets that intersect between the four comparison groups (**Figure 2B**), and displaying the expression values derived from the two comparison groups, brain metastatic PTC *vs*. non-brain metastatic PTCs and brain metastatic PTC (TR) *vs*. non-brain metastatic PTCs (Supplement Table 1). Molecules that are comparably upregulated in the brain metastatic PTC include CCL2, CCL13, CCL18, CCL20, CCL22, CXCL1, CXCL2, CXCL8, CXCL14, CX3CL1, CLDN10, FPR2, IL1A, IL1B, IL1R2, ICAM1, and MMP7. SDC2 is comparably downregulated. A number of molecules from the probe sets are displayed under their group specific names, e.g. chemokines, CLDN, fMLPR, IL-1, MMP, and SDC. This pathway was also most significantly associated with the 95 probe sets (*p*-value 5.51E-08).

upregulation of CCL20 in endothelial cells that line specific zones of the BBB has been associated with a support for autoreactive T cells to cross the BBB regionally [24]. *CCL20* was also included in the top scoring gene list derived from a comparison of parental breast cancer cell lines CN34 and MDA231 with their derivatives possessing brain metastatic behavior [25]. CXCL1 and CXCL2 are neutrophil chemoattractants. Overexpression of both chemokines in breast cancer cells increased survival of cancer cells at the metastatic sites [26]. In a rat model of soman-induced status epilepticus, CXCL1 expression was induced in neurons and endothelial cells [27]. An *in vitro* and *in vivo* study demonstrated that CCL2 expression from breast cancer cells and stroma attracts inflammatory monocytes that promotes metastasis of breast tumors [28]. CCL13 is the ligand of chemokine receptors CCR1, CCR2, CCR3, and CCR5. Although CCL13 is a critical factor in inflammatory diseases [29] its functions in cancer is not well defined. OSM is structurally related to IL6 and was found to inhibit thyroid peroxidase gene expression in porcine thyroid cell culture [30]. CXCL8, IL17, and IL6 were among a number of cytokines that were detected with increased levels upon neuroinflammatory stimulus in a 3D microfluidic chip model of the human BBB [31]. Furthermore, in SW480 and Caco-2 cells, proliferation, invasion, or epithelial-mesenchymal transition could be synergistically fostered by CXCL8 and CCL20 via the PI3K/AKT and ERK1/2 pathways [32]. GBM cells which were selected in a lung metastasis assay showed increased expression of IL6, IL8 and other factors known to be associated with unfavorable prognosis [33]. IL17C is preferentially expressed from non-immune cells and its expression was found to be comparably upregulated in the CNS of mice with induced autoimmune encephalomyelitis [34, 35]. In an *in vitro* BBB model, treatment with recombinant IL1B abolished BBB integrity by suppressing astrocytic SHH production and furthermore, led to increased synthesis of CCL2, CCL20, and CXCL2 in astrocytes [36]. The proinflammatory cytokine IL32, alias NK4, is an established cancer associated factor that was demonstrated e.g. in cell culture experiments wherein a splice variant of IL32 promoted migration and invasion of breast cancer cells via the downstream VEGF/STAT3 pathway [37].

Proteins with receptor activity

IL1R2 is a decoy receptor that interferes with the binding of IL1R1 to IL1A and IL1B. The receptor is known to be expressed in various cancer types [38]. *ROS1* encodes a receptor tyrosine kinase with yet unknown ligand and it exhibits conserved relationship with *ALK* and the leukocyte tyrosine kinase *LTK*. Among other genes, upregulation of ROS1 was detected in GBM clones that were resistant to the EGFR inhibitor Gefitinib [39]. FPR2 is a G protein-coupled chemoattractant receptor [40]. *In vitro* and in *vivo* studies revealed that glioma cells overexpressing FPR showed increased motility and were more invasive than non-FPR overexpressing glioma cells [41]. SIGLEC6 is a cell membrane receptor containing an extracellular immunoglobulin domain for sialic acids binding and an intracellular immunoreceptor tyrosine-based inhibitory motif. Expression of *SIGLEC6* in choriocarcinoma-derived BeWO cells resulted in decreased apoptosis and enhanced proliferation and invasiveness [42].

Cytoskeletal and related proteins

MYBPH is a cytoskeletal protein that is involved in a number of cellular processes; however, its functions are not fully explored yet. Of notice, *in vitro* experiments demonstrated that *MYBPH* expression is positively regulated by TTF-1 and furthermore, *MYBPH* overexpression impairs actomyosin organization and acts as a negative factor for cell motility and migration of collective cells but not of single cells [43]. This latter observation can be of relevance in the context

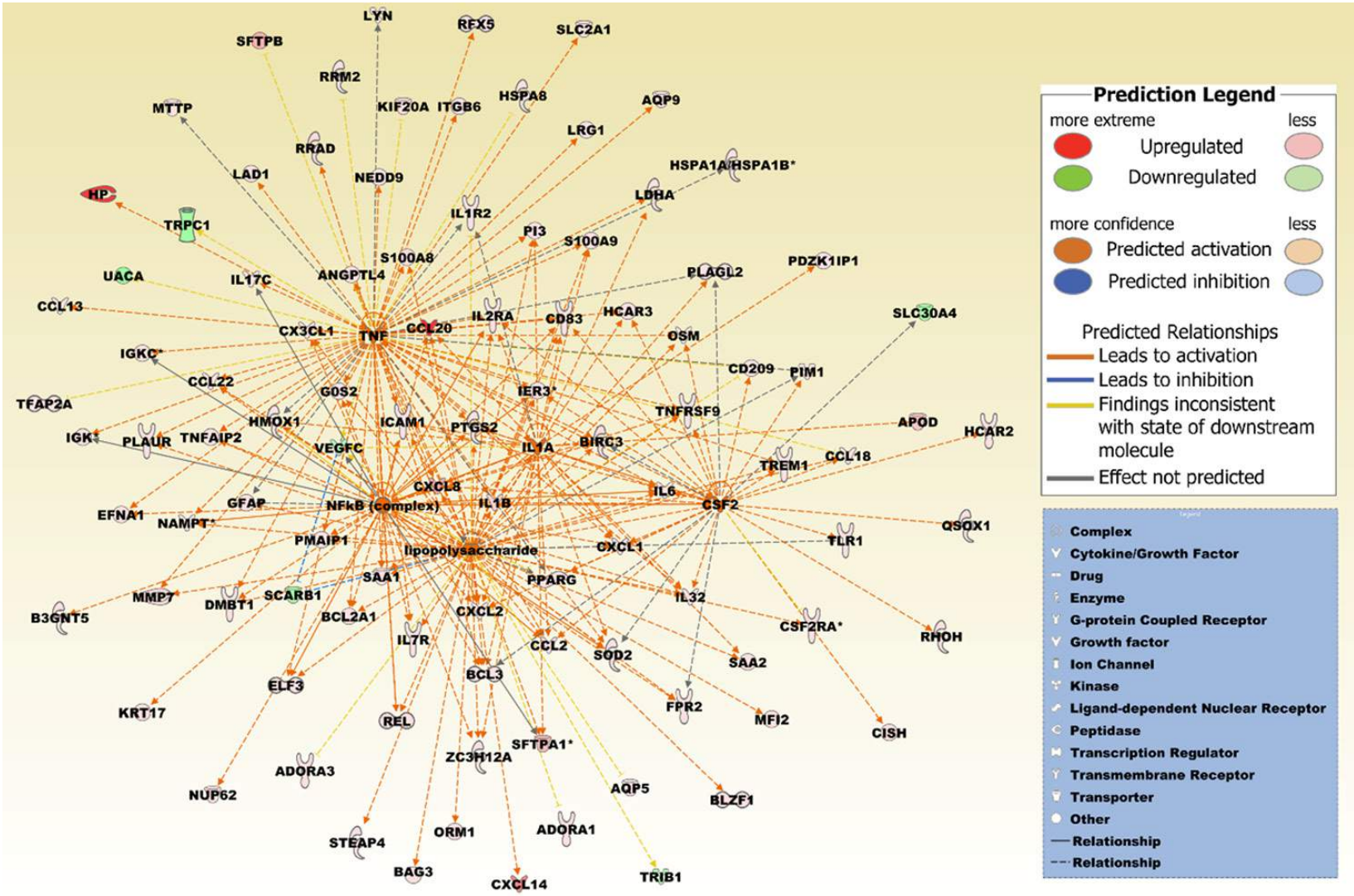

Figure 9. A merged network based on the top five upstream regulators lipopolysaccharide, nuclear NFkB (complex) and the cytokines TNF, IL1A, and CSF2. IL1A is also included in the differentially expressed probe set list. Increased activation is predicted by a z-score > 2 (**Table 3**). The network is based on the list of 429 differentially expressed probe sets that intersect between the four comparison groups (**Figure 5B**), and reflecting the expression values derived from the two comparison groups, brain metastatic PTC *vs*. non-brain metastatic PTCs and brain metastatic PTC (TR) *vs*. non-brain metastatic PTCs (Supplement Table 1). Upregulated molecules include ADORA1, ADORA3, ANGPTL4, APOD, AQP5, AQP9, B3GNT5, BAG3, BCL2A1, BCL3, BIRC3, BLZF1, CCL13, CCL18, CCL2, CCL20, CCL22, CD209, CD83, CISH, CSF2RA, CX3CL1, CXCL1, CXCL14, CXCL2, CXCL8, DMBT1, EFNA1, ELF3, FPR2, G0S2, GFAP, HCAR2, HCAR3, HMOX1, HP, HSPA1A/HSPA1B, HSPA8, ICAM1,

IER3, IGK, IGKC, IL17C, IL1A, IL1B, IL1R2, IL2RA, IL32, IL6, IL7R, ITGB6, KIF20A, KRT17, LAD1, LDHA, LRG1, LYN, MFI2, MMP7, MTTP, NAMPT, NEDD9, NUP62, ORM1, OSM, PDZK1IP1, PI3, PIM1, PLAGL2, PLAUR, PMAIP1, PPARG, PTGS2, QSOX1, REL, RFX5, RHOH, RRAD, RRM2, S100A8, S100A9, SAA1, SAA2, SFTPA1, SFTPB, SLC2A1, SOD2, STEAP4, TFAP2A, TLR1, TNFAIP2, TNFRSF9, TREM1, and ZC3H12A. Downregulated molecules include SCARB1, SLC30A4, TRIB1, TRPC1, UACA, and VEGFC. The pathway was overlaid with the Molecule Activity Predictor to precalculate further molecular effects, as outlined in the prediction legend.

that the brain metastatic cells in our study harbored expression signatures related to granulocyte/agranulocyte adhesion and diapedesis processes. GFAP is an intermediate filament protein that is an established marker for a number of glial tumors [44]. Overexpression of KRT17 has been found in an IHC study to be associated with lymph node metastasis in PTCs [45]. Within the cytoskeleton structures, actin filaments form dynamic networks that can rapidly reorganize, determine cytokinesis, cell shape, and are mandatory for cell adhesion, migration, and invasion [46]. Overexpression of the ubiquitously expressed gene *ACTBL2*, alias kappa-actin, is associated with unfavorable prognosis in hepatocellular carcinoma and its induced overexpression in hepatoma cells led to enhanced serum-independent cell proliferation and anchorage-independent colony formation [47]. Expressional dataset analysis detected overexpression of the beta tubulin protein TUBB3 in brain metastases of breast cancers but not in the primary tumors [48]. Furthermore, knockdown of TUBB3 in brain metastatic breast cancer cells reduced their metastatic capacity in mice which led to increased survival of the rodents.

Enzymes including proteases and their inhibitors

XDH encodes a molybdoflavin enzyme that catalyzes the oxidative reactions of hypoxanthine to xanthine and subsequently of xanthine to uric acid. The role of the enzyme in cancer has not been thoroughly elucidated; however, XDH expression has been identified by mass spectrometry in bovine brain capillary endothelial cells (BCECs) exhibiting functional BBB properties that were induced by co-cultured glial cells, whereas mono-cultured BCECs with impaired BBB properties did not express detectable XDH [49]. PI3, also known as elafin, is a serine protease inhibitor that is synthesized and secreted locally at the site of injury in response to primary cytokines such as IL1 and TNF [50]. In an experimental anti-angiogenesis *in vivo* model system, PI3 was upregulated in GBM and its upregulation was found to be associated with poor prognosis in GBM patients [51]. *NAPSA* encodes an aspartic protease that is used as an IHC marker for subclassification of lung tumors. In thyroid cancer, IHC expression of *NAPSA* was detected in a subset of poorly differentiated thyroid carcinomas and anaplastic carcinomas but only in a vast minority of PTCs [52]. FSTL5 is an enzyme modulator of the follistatin family and the secretory glycoprotein was identified in a microarray expression and IHC study as a marker of unfavourable prognosis in different subtypes of medulloblastomas [53]. The function of SPINK14 in cancer is barely known but the protease inhibitor was listed among the top downregulated genes in HepG2 cells upon treatment with the EZH2 inhibitor GSK343 [54]. TMPRSS3 is a type II transmembrane serine protease that, when overexpressed in ovarian A2780 cells, promotes their proliferation, invasion, and migration and an IHC study revealed that TMPRSS3 expression is an unfavorable prognostic factor in breast cancer patients [55, 56]. MMP7 is a secreted matrix metalloproteinase. *In vitro* assays in prostate cancer cells demonstrated that the proteinase sufficiently digests perlecan, a core component of basement membranes, and by this facilitates cell invasion [57].

Transporter proteins

The vesicular acetylcholine transporter SLC-18A3 encodes a transmembrane molecule that loads acetylcholine into secretory vesicles in presynaptic nerve terminals. An RT-PCR assay demonstrated that induction of differentiation of human neuroblastoma cell line LAN-5 by retinoic acid resulted in a number of deregulated genes under which SLC18A3 was shown to be initially upregulated [58]. CP owns ferroxidase activity and it is implicated in supporting iron transport across the BBB. In an *in vitro* BBB model system, expression of CP in C6 glioma cells was stimulated by IL1B and IL6 that were expressed from neighboring brain microvascular endothelial cells [59]. According to microarray expression data, CNTNAP5, which is a

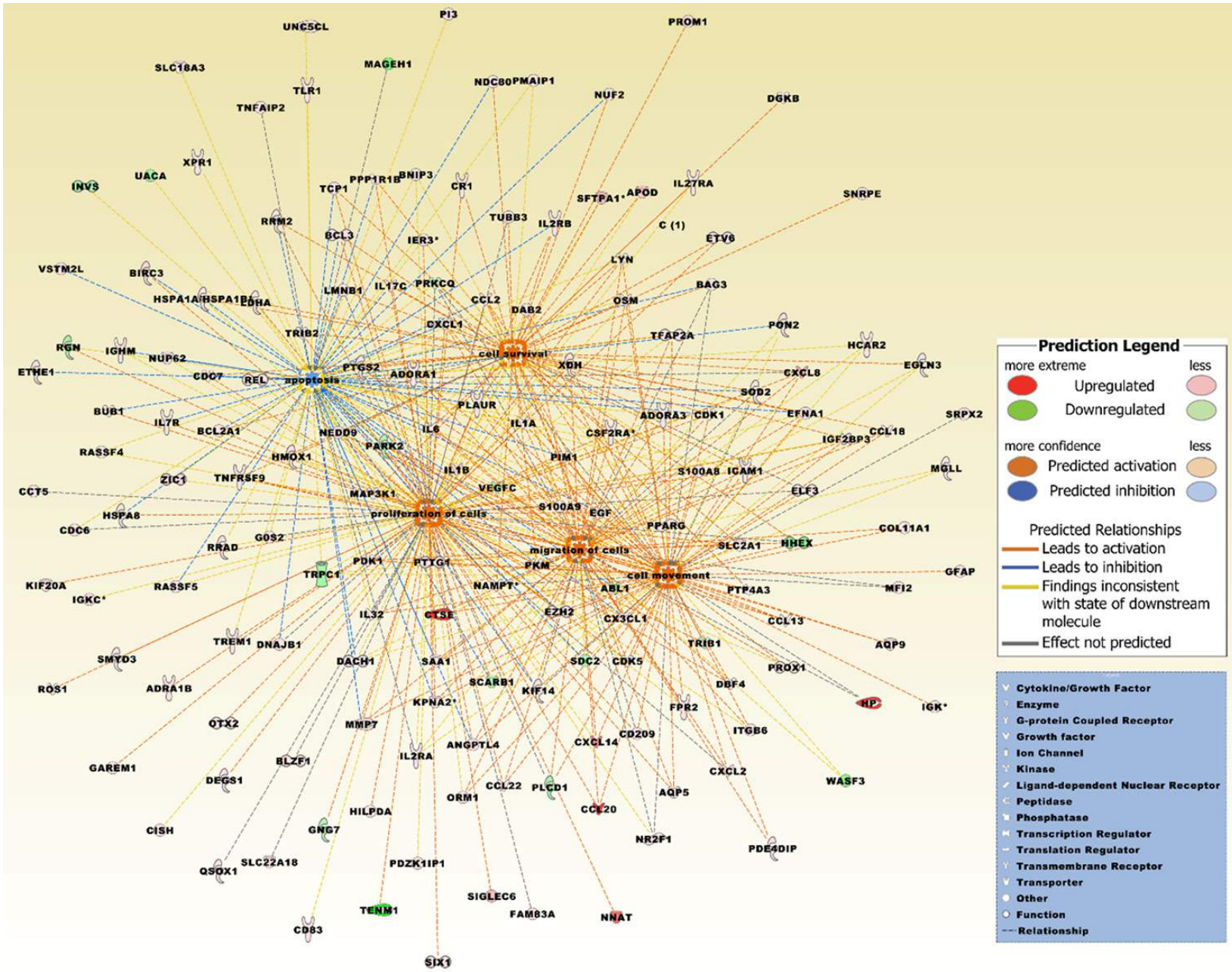
Prediction Legend
more extreme
less
Upregulated
Downregulated
more confidence
less
Predicted activation
Predicted inhibition
Predicted Relationships
Leads to activation
Leads to inhibition
Findings inconsistent with state of downstream molecule
Effect not predicted
Cytokine/Growth Factor
Enzyme
G-protein Coupled Receptor
Growth factor
Ion Channel
Kinase
Ligand-dependent Nuclear Receptor
Peptidase
Phosphatase
Transcription Regulator
Translation Regulator
Transmembrane Receptor
Transporter
Other
Function
Relationship
cell survival
apoptosis
proliferation of cells
migration of cells
cell movement
PI3
UNC5CL
PROM1
SLC18A3
MAGEH1
TLR1
NDC80
PMAIP1
NUF2
DGKB
TNFAIP2
XPR1
UACA
INVS
PPP1R15B
BNIP3
TCP1
CR1
SFTPA1
APOD
IL27RA
SNRPE
RRM2
TUBB3
IL2RB
C (1)
BCL3
IER3
ETV6
LYN
VSTM2L
BIRC3
LMNB1
IL17C
PRKCQ
BAG3
HSPA1A
HSPA1B
EDHA
CCL2
DAB2
OSM
TRIB2
CXCL1
PON2
TFAP2A
RGN
IGHM
NUP62
HCAR2
ETHE1
CDO7
REL
PTGS2
ADORA1
XDH
EGLN3
CXCL8
SOD2
PLAUR
BUB1
IL7R
BCL2A1
NEDD9
IL6
IL1A
ADORA3
CDK1
EFNA1
SRPX2
CSF2RA
CCL18
IGF2BP3
RASSF4
PARK2
HMOX1
PIM1
IL1B
S100A8
IGAM1
MGLL
ZIC1
TNFRSF9
CCT5
MAP3K1
VEGFC
ELF3
HSPA8
S100A9
EGF
CDC6
PPARG
COL11A1
GOS2
RRAD
SLC2A1
HHEX
PDK1
PTTG1
PKM
TRPC1
GFAP
KIF20A
RASSF5
NAMPT
ABL1
PTP4A3
MFI2
IGKC
IL32
CTSE
EZH2
CX3CL1
CCL13
TREM1
DNAJB1
TRIB1
AQP9
SMYD3
DACH1
SAA1
SDC2
CDK5
PROX1
ROS1
ADRA1B
SCARB1
KIF14
DBF4
KPNA2
HP
IGK
FPR2
OTX2
MMP7
CD209
ITGB6
ANGPTL4
CXCL14
IL2RA
GAREM1
BLZF1
CXCL2
DEGS1
CCL22
PLCD1
AQP5
WASF3
ORM1
HILPDA
CCL20
CISH
GNG7
NR2F1
PDE4DIP
QSOX1
SLC22A18
PDZK1IP1
SIGLEC6
TENM1
FAM83A
NHAT
CD83
SIX1

Figure 10. The top five merged networks under the category diseases & functions were entitled migration of cells, cell movement, cell survival, apoptosis, and proliferation of cells. Increased activation is predicted by a z-score > 2 (**Table 3**). The network is based on the list of 429 differentially expressed probe sets that intersect between the four comparison groups (**Figure 5B**), and reflecting the expression values derived from the two comparison groups, brain metastatic PTC *vs*. non-brain metastatic PTCs and brain metastatic PTC (TR) *vs*. non-brain metastatic PTCs (Supplement Table 1). Upregulated molecules include ADORA1, ADORA3, ADRA1B, ANGPTL4, APOD, AQP5, AQP9, BAG3, BCL2A1, BCL3, BIRC3, BLZF1, BNIP3, BUB1, CCL13, CCL18, CCL2, CCL20, CCL22, CCT5, CD209, CD83, CDC6, CDC7, CDK1, CDK5, CISH, COL11A1, CR1, CSF2RA, CTSE, CX3CL1, CXCL1, CXCL14, CXCL2, CXCL8, DAB2, DACH1, DBF4, DEGS1, DGKB, DNAJB1, EFNA1, EGF, EGLN3, ELF3, ETHE1, ETV6, EZH2, FAM83A, FPR2, G0S2, GAREM1, GFAP, HCAR2, HILPDA, HMOX1, HP, HSPA1A/HSPA1B, HSPA8, ICAM1, IER3, IGF2BP3, IGHM, IGK, IGKC, IL17C, IL1A, IL1B, IL27RA, IL2RA, IL2RB, IL32, IL6, IL7R, ITGB6, KIF14, KIF20A, KPNA2, LDHA, LMNB1, LYN, MAP3K1, MFI2, MGLL, MMP7, NAMPT, NDC80, NEDD9, NNAT, NR2F1, NUF2, NUP62, ORM1, OSM, OTX2, PDE4DIP, PDK1, PDZK1IP1, PI3, PIM1, PKM, PLAUR, PMAIP1, PON2, PPARG, PPP1R1B, PROM1, PROX1, PTGS2, PTP4A3, PTTG1, QSOX1, RASSF4, RASSF5, REL, ROS1, RRAD, RRM2, S100A8, S100A9, SAA1, SFTPA1, SIGLEC6, SIX1, SLC18A3, SLC22A18, SLC2A1, SMYD3, SNRPE, SOD2, SRPX2, TCP1, TFAP2A, TLR1, TNFAIP2, TNFRSF9, TREM1, TRIB2, TUBB3, UNC5CL, VSTM2L, XDH, XPR1, and ZIC1. Downregulated molecules include ABL1, GNG7, HHEX, INVS, MAGEH1, PARK2, PLCD1, PRKCQ, RGN, SCARB1, SDC2, TENM1, TRIB1, TRPC1, UACA, VEGFC, and WASF3. The pathway was overlaid with the Molecule Activity Predictor to precalculate further molecular effects, as outlined in the prediction legend.

member of the neurexin family and associated with potassium channels is comparably high expressed in a number of brain cancers including medulloblastoma, pilocytic astrocytoma, and cerebellar tumors [60]. In prostate cancer, the water channel protein AQP5 was identified as an unfavorable prognostic marker and cell culture experiments indicated that siRNA knockdown of AQP5 inhibited proliferation and migration of prostate cancer cells [61].

Molecules of various categories

HP has been found with increased serum levels by quantitative protein analysis in patients with brain metastatic lung cancer [62]. Furthermore, *in vitro* and *in vivo* studies identified HP as a key mediator of metastatic cell homing, fostering invasion, migration, including transendothelial migration, and proliferation of cancer cells [63]. SAA proteins are the major acute phase response molecules and considered as a family of apolipoproteins. SAA2-SAA4 is transcripted as a readthrough between the adjunct SAA2 and SAA4 genes. Overexpression of isoforms SAA1 and SAA2 was found in sera of lung cancer patients and in lung carcinoma cells that metastasized and settled in the lung of a mouse model [64]. Furthermore, recombinant SAA1 differentially affected cell migration and invasion in two tested glioma cell lines [65]. DMBT1 is a member of the scavenger receptor cysteine-rich superfamily and it was initially identified as a gene deleted in a number of medulloblastoma and GBM samples and cell lines [66]. Detailed *in vitro* and *in vivo* studies established DMBT1 as a critical vascular extracellular matrix protein that promotes endothelial cell adhesion, migration, proliferation, and angiogenesis [67]. *ZER1*, that was in our study comparably downregulated in the brain metastatic PTC, encodes a subunit of an E3 ubiquitin ligase complex. A microarray study in bladder cancer identified, among other genes, upregulation of *ZER1* at tumor stage Ta-T1; however, its downregulation at stage T1-T2 [68]. Upon heat induction, heat shock protein HSPA6 has been identified in centrioles that are known to have critical functions in cellular polarity and migration processes during neuronal differentiation [69]. *OTX2* encodes a homeobox transcription factor and is frequently gained in non-Shh/non-Wnt medulloblastomas. *In vitro* and *in vivo* experiments demonstrated that OTX2 overexpression promotes cell proliferation, whereas its knockdown reduces tumorigenicity of cells [70]. *RRAD* is a member of the (Rem/Rem2, Gem, Kir) RGK subfamily of the Ras family of small GTPases, sharing in its GTPase domain a ~35% identity with HRAS and other small GTPases. Overexpression of *RRAD* in primary GBM is associated with poor prognosis [71]. Furthermore, cell culture experiments in GBM LN229 cells demonstrated that RRAD, by inducing EGF, enhances STAT3 activation. Furthermore, immunoprecipitation showed that RRAD physically interacts with EGFR and *in vitro* and *in vivo* studies demonstrated that RRAD enhances colony formation and cell migration as well as tumor growth in nude mice. Downregulation of RRAD by siRNA treatment resulted in loss of expression of the stemness-regulating genes *OCT4*, *NANOG*, and *SOX2* as well as in sensitizing of otherwise temozolomide-resistant LN229 clones. The small GTPase Rab7b is known to be involved in retrograde

transport of a number of sorting receptors and implicated in cell migration by actin cytoskeletal remodelling [72]. In a spinal cord injury rat model, MiR146A was one of the key miRNAs that was upregulated at the injury site over a longer time period and cell culture experiments indicated that MIR146A is a regulator of inflammation in glial cells [73, 74]. SBSN is known as an invasion promoting protein that was identified in a proteomics study in the secretome of a GBM cell line that does not express EGFR and PTEN and in GBM derivate cells that have induced expression of both, EGFR and PTEN [75]. In mouse tumor endothelial cells, siRNA depletion of SBSN inhibited migration and tube formation capacity [76]. The functional properties of *FAM83A* are less known, however, its overexpression in breast cancer cells increased proliferation and invasion and augmented EGFR resistance to tyrosine kinase inhibitors [77]. Moreover, independently of an upstream EGF/EGFR activation, FAM83A overexpression resulted in activation of CRAF and PI3K p85 which are known upstream activators of ERK1/2 and AKT. Conversely, FAM83A depletion by siRNA resulted in delayed tumor growth of a xenograft tumor model and metadata analysis demonstrated that high *FAM83A* expression correlates with unfavorable prognosis in breast cancer patients.

Probe sets differentially expressed in the brain metastatic PTC, the TR, and primary brain tumors vs. non-brain metastatic PTCs

C1R is a serine protease of the complement system and an activator of C1S that is known to enhance tumorigenic invasion and migration by extracellular matrix disintegration [78]. CASP1 and CASP4 are effector caspases that are involved in caspase activation and regulation of inflammatory processes [79]. Comparably highest RNA expression levels for WDR72, which is a critical factor in calcium transport, have been found in kidney and thyroid tissues which may support our results showing lower expression of *WDR72* in the brain metastatic PTC and primary brain tumors [80]. The function of CC2D2B, especially in cancer, is virtually unknown; however, microarray expression data indicated that *CC2D2B* is a top upregulated gene in PTCs which may also be a support for our results of comparably lower expression of the factor in the brain metastasis and primary brain tumors [60]. Similarly, *CITED1* which encodes a CREB-binding protein/p300-interacting transactivator was identified in a microarray expression study as an upregulated gene in PTCs [81]. ZHX2 is a zinc finger and homeobox containing factor. Induced expression of ZHX2 in xenograft tumors resulted in reduced tumor growths [82].

In conclusion, whole transcript expression profiling identified candidate genes including a number of cytokines, and biofunctions, notably the granulocyte adhesion and diapedesis pathway, associated with a brain metastasis of a PTC, suggesting an inherited expression profile related to the brain metastatic process.

Acknowledgements

This study was supported by King Abdulaziz City for Science and Technology (KACST) grant AT-32-98 and KACST Technology Innovation Center in Personalized Medicine grant 13-CIPM-07. We thank Alaa Alamdi, Reem Alotibi, Nadia Baqtian, Ohoud Subhi, Manal Shabaat, Ishaq Khan, Mona Al-Omary, Nawal Madkhali, Lobna Siraj Mira, Maha Al-Quaiti, Fai Ashgan, Alaa Ghazi Almasri, Sabrin Bukhari, and Shireen Hussain for excellent technical assistance.

Disclosure of conflict of interest

None.

Abbreviations

aCGH, array comparative genomic hybridization; BBB, blood brain barrier; FC, fold change; FDR, false discovery rate; GO, gene ontology; GBM, glioblastoma multiforme; IHC, immunohistochemistry; FVPTC, follicular variant of PTC; PCA, principal component analysis; PTC, papillary thyroid carcinoma; TR, technical replicate.

Address correspondence to: Dr. Hans-Juergen Schulten, Center of Excellence in Genomic Medicine Research, King Abdulaziz University, Jeddah 21589, Saudi Arabia. E-mail: hschulten@kau.edu.sa

References

[1] Zecchin D, Boscaro V, Medico E, Barault L, Martini M, Arena S, Cancelliere C, Bartolini A, Crowley EH, Bardelli A, Gallicchio M and Di Nicolantonio F. BRAF V600E is a determinant of sensitivity to proteasome inhibitors. Mol Cancer Ther 2013; 12: 2950-2961.

[2] Schulten HJ, Alotibi R, Al-Ahmadi A, Ata M, Karim S, Huwait E, Gari M, Al-Ghamdi K, Al-Mashat F, Al-Hamour O, Al-Qahtani MH and Al-Maghrabi J. Effect of BRAF mutational status on expression profiles in conventional papillary thyroid carcinomas. BMC Genomics 2015; 16 Suppl 1: S6.

[3] Dadu R and Cabanillas ME. Optimizing therapy for radioactive iodine-refractory differentiated thyroid cancer: current state of the art and future directions. Minerva Endocrinol 2012; 37: 335-356.

[4] Tahmasebi FC, Farmer P, Powell SZ, Aldape KD, Fuller GN, Patel S, Hollis P, Chalif D, Eisenberg MB and Li JY. Brain metastases from papillary thyroid carcinomas. Virchows Arch 2013; 462: 473-480.

[5] Tsuda K, Tsurushima H, Takano S, Tsuboi K and Matsumura A. Brain metastasis from papillary thyroid carcinomas. Mol Clin Oncol 2013; 1: 817-819.

[6] Chiu AC, Delpassand ES and Sherman SI. Prognosis and treatment of brain metastases in thyroid carcinoma. J Clin Endocrinol Metab 1997; 82: 3637-3642.

[7] Shen Y, Ruan M, Luo Q, Yu Y, Lu H, Zhu R and Chen L. Brain metastasis from follicular thyroid carcinoma: treatment with sorafenib. Thyroid 2012; 22: 856-860.

[8] Singh M, Manoranjan B, Mahendram S, McFarlane N, Venugopal C and Singh SK. Brain metastasis-initiating cells: survival of the fittest. Int J Mol Sci 2014; 15: 9117-9133.

[9] Wilhelm I, Molnar J, Fazakas C, Hasko J and Krizbai IA. Role of the blood-brain barrier in the formation of brain metastases. Int J Mol Sci 2013; 14: 1383-1411.

[10] AJCC Cancer Staging Manual. Edited by Edge SB, Byrd DR, Compton CC, Fritz AG, Greene FL, Trotti A. New York: Springer; 2010.

[11] Schulten HJ, Hussein D, Al-Adwani F, Karim S, Al-Maghrabi J, Al-Sharif M, Jamal A, Al-Ghamdi F, Baeesa SS, Bangash M, Chaudhary A and Al-Qahtani M. Microarray Expression Data Identify DCC as a Candidate Gene for Early Meningioma Progression. PLoS One 2016; 11: e0153681.

[12] Schneider CA, Rasband WS and Eliceiri KW. NIH Image to ImageJ: 25 years of image analysis. Nat Methods 2012; 9: 671-675.

[13] Schulten HJ, Salama S, Al-Mansouri Z, Alotibi R, Al-Ghamdi K, Al-Hamour OA, Sayadi H, Al-Aradati H, Al-Johari A, Huwait E, Gari M, Al-Qahtani MH and Al-Maghrabi J. BRAF mutations in thyroid tumors from an ethnically diverse group. Hered Cancer Clin Pract 2012; 10: 10.

[14] Schulten HJ, Al-Mansouri Z, Baghallab I, Bagatian N, Subhi O, Karim S, Al-Aradati H, Al-Mutawa A, Johary A, Meccawy AA, Al-Ghamdi K, Al-Hamour O, Al-Qahtani M and Al-Maghrabi J. Comparison of microarray expression profiles between follicular variant of papillary thyroid carcinomas and follicular adenomas of the thyroid. BMC Genomics 2015; 16 Suppl 1: S7.

[15] Schulten HJ, Alotibi R, Al-Ahmadi A, Ata M, Karim S, Huwait E, Gari M, Al-Ghamdi K, Al-Mashat F, Al-Hamour O, Al-Qahtani M and Al-Maghrabi J. Effect of BRAF mutational status on expression profiles in conventional papillary thyroid carcinomas. BMC Genomics 2015; 16 Suppl 1: S6.

[16] Mi H, Poudel S, Muruganujan A, Casagrande JT and Thomas PD. PANTHER version 10: expanded protein families and functions, and analysis tools. Nucleic Acids Res 2016; 44: D336-342.

[17] Schulten HJ, Al-Mansouri Z, Baghallab I, Bagatian N, Subhi O, Karim S, Al-Aradati H, Al-Mutawa A, Johary A, Meccawy AA, Al-Ghamdi K, Al-Hamour O, Al-Qahtani MH and Al-Maghrabi J. Comparison of microarray expression profiles between follicular variant of papillary thyroid carcinomas and follicular adenomas of the thyroid. BMC Genomics 2015; 16 Suppl 1: S7.

[18] Kramer A, Green J, Pollard J Jr and Tugendreich S. Causal analysis approaches in Ingenuity Pathway Analysis. Bioinformatics 2014; 30: 523-530.

[19] Al-Dhahri SF, Al-Amro AS, Al-Shakwer W and Terkawi AS. Cerebellar mass as a primary presentation of papillary thyroid carcinoma: case report and literature review. Head Neck Oncol 2009; 1: 23.

[20] El-Osta H, Falchook G, Tsimberidou A, Hong D, Naing A, Kim K, Wen S, Janku F and Kurzrock R. BRAF mutations in advanced cancers: clinical characteristics and outcomes. PLoS One 2011; 6: e25806.

[21] Capper D, Berghoff AS, Magerle M, Ilhan A, Wohrer A, Hackl M, Pichler J, Pusch S, Meyer J, Habel A, Petzelbauer P, Birner P, von Deimling A and Preusser M. Immunohistochemical testing of BRAF V600E status in 1,120 tumor tissue samples of patients with brain metastases. Acta Neuropathol 2012; 123: 223-233.

[22] Tufano RP, Teixeira GV, Bishop J, Carson KA and Xing M. BRAF mutation in papillary thyroid cancer and its value in tailoring initial treatment: a systematic review and meta-analysis. Medicine (Baltimore) 2012; 91: 274-286.

[23] Zeng W, Chang H, Ma M and Li Y. CCL20/CCR6 promotes the invasion and migration of thyroid cancer cells via NF-kappa B signaling-induced MMP-3 production. Exp Mol Pathol 2014; 97: 184-190.

[24] Arima Y, Harada M, Kamimura D, Park JH, Kawano F, Yull FE, Kawamoto T, Iwakura Y, Betz UA, Marquez G, Blackwell TS, Ohira Y, Hirano T and Murakami M. Regional neural activation

defines a gateway for autoreactive T cells to cross the blood-brain barrier. Cell 2012; 148: 447-457.
[25] Bos PD, Zhang XH, Nadal C, Shu W, Gomis RR, Nguyen DX, Minn AJ, van de Vijver MJ, Gerald WL, Foekens JA and Massague J. Genes that mediate breast cancer metastasis to the brain. Nature 2009; 459: 1005-1009.
[26] Acharyya S, Oskarsson T, Vanharanta S, Malladi S, Kim J, Morris PG, Manova-Todorova K, Leversha M, Hogg N, Seshan VE, Norton L, Brogi E and Massagué J. A CXCL1 paracrine network links cancer chemoresistance and metastasis. Cell 2012; 150: 165-178.
[27] Johnson EA, Dao TL, Guignet MA, Geddes CE, Koemeter-Cox AI and Kan RK. Increased expression of the chemokines CXCL1 and MIP-1alpha by resident brain cells precedes neutrophil infiltration in the brain following prolonged soman-induced status epilepticus in rats. J Neuroinflammation 2011; 8: 41.
[28] Qian BZ, Li J, Zhang H, Kitamura T, Zhang J, Campion LR, Kaiser EA, Snyder LA and Pollard JW. CCL2 recruits inflammatory monocytes to facilitate breast-tumour metastasis. Nature 2011; 475: 222-225.
[29] Mendez-Enriquez E and Garcia-Zepeda EA. The multiple faces of CCL13 in immunity and inflammation. Inflammopharmacology 2013; 21: 397-406.
[30] Isozaki O, Tsushima T, Miyakawa M, Emoto N, Demura H, Arai M and Sato-Nozoe Y. Oncostatin M: a new potent inhibitor of iodine metabolism inhibits thyroid peroxidase gene expression but not DNA synthesis in porcine thyroid cells in culture. Thyroid 1997; 7: 71-77.
[31] Herland A, van der Meer AD, FitzGerald EA, Park TE, Sleeboom JJ and Ingber DE. Distinct Contributions of Astrocytes and Pericytes to Neuroinflammation Identified in a 3D Human Blood-Brain Barrier on a Chip. PLoS One 2016; 11: e0150360.
[32] Cheng XS, Li YF, Tan J, Sun B, Xiao YC, Fang XB, Zhang XF, Li Q, Dong JH, Li M, Qian HH, Yin ZF and Yang ZB. CCL20 and CXCL8 synergize to promote progression and poor survival outcome in patients with colorectal cancer by collaborative induction of the epithelial-mesenchymal transition. Cancer Lett 2014; 348: 77-87.
[33] Xie Q, Thompson R, Hardy K, DeCamp L, Berghuis B, Sigler R, Knudsen B, Cottingham S, Zhao P, Dykema K, Cao B, Resau J, Hay R and Vande Woude GF. A highly invasive human glioblastoma pre-clinical model for testing therapeutics. J Transl Med 2008; 6: 77.
[34] Waisman A, Hauptmann J and Regen T. The role of IL-17 in CNS diseases. Acta Neuropathol 2015; 129: 625-637.
[35] Chang SH, Reynolds JM, Pappu BP, Chen G, Martinez GJ and Dong C. Interleukin-17C promotes Th17 cell responses and autoimmune disease via interleukin-17 receptor E. Immunity 2011; 35: 611-621.
[36] Wang Y, Jin S, Sonobe Y, Cheng Y, Horiuchi H, Parajuli B, Kawanokuchi J, Mizuno T, Takeuchi H and Suzumura A. Interleukin-1beta induces blood-brain barrier disruption by downregulating Sonic hedgehog in astrocytes. PLoS One 2014; 9: e110024.
[37] Park JS, Choi SY, Lee JH, Lee M, Nam ES, Jeong AL, Lee S, Han S, Lee MS, Lim JS, Yoon do Y, Kwon Y and Yang Y. Interleukin-32beta stimulates migration of MDA-MB-231 and MCF-7cells via the VEGF-STAT3 signaling pathway. Cell Oncol (Dordr) 2013; 36: 493-503.
[38] Liu X, Min L, Duan H, Shi R, Zhang W, Hong S and Tu C. Short hairpin RNA (shRNA) of type 2 interleukin-1 receptor (IL1R2) inhibits the proliferation of human osteosarcoma U-2 OS cells. Med Oncol 2015; 32: 364.
[39] Aljohani H, Koncar RF, Zarzour A, Park BS, Lee SH and Bahassi el M. ROS1 amplification mediates resistance to gefitinib in glioblastoma cells. Oncotarget 2015; 6: 20388-20395.
[40] Huang J, Chen K, Gong W, Zhou Y, Le Y, Bian X and Wang JM. Receptor "hijacking" by malignant glioma cells: a tactic for tumor progression. Cancer Lett 2008; 267: 254-261.
[41] Huang J, Chen K, Chen J, Gong W, Dunlop NM, Howard OM, Gao Y, Bian XW and Wang JM. The G-protein-coupled formylpeptide receptor FPR confers a more invasive phenotype on human glioblastoma cells. Br J Cancer 2010; 102: 1052-1060.
[42] Rumer KK, Post MD, Larivee RS, Zink M, Uyenishi J, Kramer A, Teoh D, Bogart K and Winn VD. Siglec-6 is expressed in gestational trophoblastic disease and affects proliferation, apoptosis and invasion. Endocr Relat Cancer 2012; 19: 827-840.
[43] Hosono Y, Yamaguchi T, Mizutani E, Yanagisawa K, Arima C, Tomida S, Shimada Y, Hiraoka M, Kato S, Yokoi K, Suzuki M and Takahashi T. MYBPH, a transcriptional target of TTF-1, inhibits ROCK1, and reduces cell motility and metastasis. EMBO J 2012; 31: 481-493.
[44] Goyal R, Mathur SK, Gupta S, Goyal R, Kumar S, Batra A, Hasija S and Sen R. Immunohistochemical expression of glial fibrillary acidic protein and CAM5.2 in glial tumors and their role in differentiating glial tumors from metastatic tumors of central nervous system. J Neurosci Rural Pract 2015; 6: 499-503.
[45] Kim HS, Lee JJ, Do SI, Kim K, Do IG, Kim DH, Chae SW and Sohn JH. Overexpression of cytokeratin 17 is associated with the development of papillary thyroid carcinoma and the pres-

ence of lymph node metastasis. Int J Clin Exp Pathol 2015; 8: 5695-5701.
[46] Simiczyjew A, Mazur AJ, Popow-Wozniak A, Malicka-Blaszkiewicz M and Nowak D. Effect of overexpression of beta- and gamma-actin isoforms on actin cytoskeleton organization and migration of human colon cancer cells. Histochem Cell Biol 2014; 142: 307-322.
[47] Chang KW, Chou A, Lee CC, Yeh C, Lai MW, Yeh TS, Chen TC, Liang KH and Yeh CT. Overexpression of kappa-actin alters growth properties of hepatoma cells and predicts poor postoperative prognosis. Anticancer Res 2011; 31: 2037-2044.
[48] Kanojia D, Morshed RA, Zhang L, Miska JM, Qiao J, Kim JW, Pytel P, Balyasnikova IV, Lesniak MS and Ahmed AU. betaIII-Tubulin Regulates Breast Cancer Metastases to the Brain. Mol Cancer Ther 2015; 14: 1152-1161.
[49] Cantu-Medellin N and Kelley EE. Xanthine oxidoreductase-catalyzed reduction of nitrite to nitric oxide: insights regarding where, when and how. Nitric Oxide 2013; 34: 19-26.
[50] Sallenave JM. The role of secretory leukocyte proteinase inhibitor and elafin (elastase-specific inhibitor/skin-derived antileukoprotease) as alarm antiproteinases in inflammatory lung disease. Respir Res 2000; 1: 87-92.
[51] Saidi A, Javerzat S, Bellahcene A, De Vos J, Bello L, Castronovo V, Deprez M, Loiseau H, Bikfalvi A and Hagedorn M. Experimental anti-angiogenesis causes upregulation of genes associated with poor survival in glioblastoma. Int J Cancer 2008; 122: 2187-2198.
[52] Chernock RD, El-Mofty SK, Becker N and Lewis JS Jr. Napsin A expression in anaplastic, poorly differentiated, and micropapillary pattern thyroid carcinomas. Am J Surg Pathol 2013; 37: 1215-1222.
[53] Remke M, Hielscher T, Korshunov A, Northcott PA, Bender S, Kool M, Westermann F, Benner A, Cin H, Ryzhova M, Sturm D, Witt H, Haag D, Toedt G, Wittmann A, Schottler A, von Bueren AO, von Deimling A, Rutkowski S, Scheurlen W, Kulozik AE, Taylor MD, Lichter P and Pfister SM. FSTL5 is a marker of poor prognosis in non-WNT/non-SHH medulloblastoma. J Clin Oncol 2011; 29: 3852-3861.
[54] Liu TP, Hong YH, Tung KY and Yang PM. In silico and experimental analyses predict the therapeutic value of an EZH2 inhibitor GSK343 against hepatocellular carcinoma through the induction of metallothionein genes. Oncoscience 2016; 3: 9-20.
[55] Zhang D, Qiu S, Wang Q and Zheng J. TMPRSS3 modulates ovarian cancer cell proliferation, invasion and metastasis. Oncol Rep 2016; 35: 81-88.
[56] Rui X, Li Y, Jin F and Li F. TMPRSS3 is a novel poor prognostic factor for breast cancer. Int J Clin Exp Pathol 2015; 8: 5435-5442.
[57] Grindel BJ, Martinez JR, Pennington CL, Muldoon M, Stave J, Chung LW and Farach-Carson MC. Matrilysin/matrix metalloproteinase-7 (MMP7) cleavage of perlecan/HSPG2 creates a molecular switch to alter prostate cancer cell behavior. Matrix Biol 2014; 36: 64-76.
[58] Guglielmi L, Cinnella C, Nardella M, Maresca G, Valentini A, Mercanti D, Felsani A and D'Agnano I. MYCN gene expression is required for the onset of the differentiation programme in neuroblastoma cells. Cell Death Dis 2014; 5: e1081.
[59] McCarthy RC and Kosman DJ. Activation of C6 glioblastoma cell ceruloplasmin expression by neighboring human brain endothelia-derived interleukins in an in vitro blood inverted question markbrain barrier model system. Cell Commun Signal 2014; 12: 65.
[60] Hruz T, Laule O, Szabo G, Wessendorp F, Bleuler S, Oertle L, Widmayer P, Gruissem W and Zimmermann P. Genevestigator v3: a reference expression database for the meta-analysis of transcriptomes. Adv Bioinformatics 2008; 2008: 420747.
[61] Li J, Wang Z, Chong T, Chen H, Li H, Li G, Zhai X and Li Y. Over-expression of a poor prognostic marker in prostate cancer: AQP5 promotes cells growth and local invasion. World J Surg Oncol 2014; 12: 284.
[62] Marchi N, Mazzone P, Fazio V, Mekhail T, Masaryk T and Janigro D. ProApolipoprotein A1: a serum marker of brain metastases in lung cancer patients. Cancer 2008; 112: 1313-1324.
[63] Aguado BA, Wu JJ, Azarin SM, Nanavati D, Rao SS, Bushnell GG, Medicherla CB and Shea LD. Secretome identification of immune cell factors mediating metastatic cell homing. Sci Rep 2015; 5: 17566.
[64] Sung HJ, Ahn JM, Yoon YH, Rhim TY, Park CS, Park JY, Lee SY, Kim JW and Cho JY. Identification and validation of SAA as a potential lung cancer biomarker and its involvement in metastatic pathogenesis of lung cancer. J Proteome Res 2011; 10: 1383-1395.
[65] Knebel FH, Albuquerque RC, Massaro RR, Maria-Engler SS and Campa A. Dual effect of serum amyloid A on the invasiveness of glioma cells. Mediators Inflamm 2013; 2013: 509089.
[66] Mollenhauer J, Wiemann S, Scheurlen W, Korn B, Hayashi Y, Wilgenbus KK, von Deimling A and Poustka A. DMBT1, a new member of the SRCR superfamily, on chromosome 10q25.3-26.1 is deleted in malignant brain tumours. Nat Genet 1997; 17: 32-39.

[67] Muller H, Hu J, Popp R, Schmidt MH, Muller-Decker K, Mollenhauer J, Fisslthaler B, Eble JA and Fleming I. Deleted in malignant brain tumors 1 is present in the vascular extracellular matrix and promotes angiogenesis. Arterioscler Thromb Vasc Biol 2012; 32: 442-448.
[68] Fang ZQ, Zang WD, Chen R, Ye BW, Wang XW, Yi SH, Chen W, He F and Ye G. Gene expression profile and enrichment pathways in different stages of bladder cancer. Genet Mol Res 2013; 12: 1479-1489.
[69] Khalouei S, Chow AM and Brown IR. Stress-induced localization of HSPA6 (HSP70B') and HSPA1A (HSP70-1) proteins to centrioles in human neuronal cells. Cell Stress Chaperones 2014; 19: 321-327.
[70] Adamson DC, Shi Q, Wortham M, Northcott PA, Di C, Duncan CG, Li J, McLendon RE, Bigner DD, Taylor MD and Yan H. OTX2 is critical for the maintenance and progression of classic medulloblastoma. Cancer Res 2010; 70: 181-191.
[71] Yeom SY, Nam DH and Park C. RRAD Promotes EGFR-Mediated STAT3 Activation and Induces Temozolomide Resistance of Malignant Glioblastoma. Mol Cancer Ther 2014; 13: 3049-3061.
[72] Distefano MB, Kjos I, Bakke O and Progida C. Rab7b at the intersection of intracellular trafficking and cell migration. Commun Integr Biol 2015; 8: e1023492.
[73] Iyer A, Zurolo E, Prabowo A, Fluiter K, Spliet WG, van Rijen PC, Gorter JA and Aronica E. MicroRNA-146a: a key regulator of astrocyte-mediated inflammatory response. PLoS One 2012; 7: e44789.
[74] Strickland ER, Hook MA, Balaraman S, Huie JR, Grau JW and Miranda RC. MicroRNA dysregulation following spinal cord contusion: implications for neural plasticity and repair. Neuroscience 2011; 186: 146-160.
[75] Sangar V, Funk CC, Kusebauch U, Campbell DS, Moritz RL and Price ND. Quantitative proteomic analysis reveals effects of epidermal growth factor receptor (EGFR) on invasion-promoting proteins secreted by glioblastoma cells. Mol Cell Proteomics 2014; 13: 2618-2631.
[76] Alam MT, Nagao-Kitamoto H, Ohga N, Akiyama K, Maishi N, Kawamoto T, Shinohara N, Taketomi A, Shindoh M, Hida Y and Hida K. Suprabasin as a novel tumor endothelial cell marker. Cancer Sci 2014; 105: 1533-1540.
[77] Lee SY, Meier R, Furuta S, Lenburg ME, Kenny PA, Xu R and Bissell MJ. FAM83A confers EGFR-TKI resistance in breast cancer cells and in mice. J Clin Invest 2012; 122: 3211-3220.
[78] Rutkowski MJ, Sughrue ME, Kane AJ, Mills SA and Parsa AT. Cancer and the complement cascade. Mol Cancer Res 2010; 8: 1453-1465.
[79] Kajiwara Y, Schiff T, Voloudakis G, Gama Sosa MA, Elder G, Bozdagi O and Buxbaum JD. A critical role for human caspase-4 in endotoxin sensitivity. J Immunol 2014; 193: 335-343.
[80] Uhlen M, Fagerberg L, Hallstrom BM, Lindskog C, Oksvold P, Mardinoglu A, Sivertsson A, Kampf C, Sjostedt E, Asplund A, Olsson I, Edlund K, Lundberg E, Navani S, Szigyarto CA, Odeberg J, Djureinovic D, Takanen JO, Hober S, Alm T, Edqvist PH, Berling H, Tegel H, Mulder J, Rockberg J, Nilsson P, Schwenk JM, Hamsten M, von Feilitzen K, Forsberg M, Persson L, Johansson F, Zwahlen M, von Heijne G, Nielsen J and Ponten F. Proteomics. Tissue-based map of the human proteome. Science 2015; 347: 1260419.
[81] Huang Y, Prasad M, Lemon WJ, Hampel H, Wright FA, Kornacker K, LiVolsi V, Frankel W, Kloos RT, Eng C, Pellegata NS and de la Chapelle A. Gene expression in papillary thyroid carcinoma reveals highly consistent profiles. Proc Natl Acad Sci U S A 2001; 98: 15044-15049.
[82] Yue X, Zhang Z, Liang X, Gao L, Zhang X, Zhao D, Liu X, Ma H, Guo M, Spear BT, Gong Y and Ma C. Zinc fingers and homeoboxes 2 inhibits hepatocellular carcinoma cell proliferation and represses expression of Cyclins A and E. Gastroenterology 2012; 142: 1559-1570, e2.

Supplement Table 1. Probe sets differentially expressed in the brain metastatic PTC including its TR *vs*. non-brain metastatic PTCs and *vs*. primary brain tumors

				Brain metastatic PTC + TR *vs*. non-brain metastatic PTCs			Brain metastatic PTC + TR *vs*. primary brain tumors		
Transcript ID	Gene symbol	Gene name/assignment	Chromosomal location	*p*-value	FDR *p*-value	Fold change	*p*-value	FDR *p*-value	Fold change
8129134	ROS1	ROS proto-oncogene 1, receptor tyrosine kinase	6q22	1.93E-14	5.61E-10	13.37	1.17E-14	3.40E-10	14.70
7923534	MYBPH	myosin binding protein H	1q32.1	1.15E-11	1.54E-07	12.96	1.30E-11	1.23E-07	12.67
8180303	--	--	11p15.1	2.11E-11	2.04E-07	75.90	2.65E-11	1.72E-07	70.76
7927502	SLC18A3	solute carrier family 18 member A3	10q11.23	1.67E-10	1.05E-06	11.46	1.96E-10	8.73E-07	11.10
7997188	HP	haptoglobin	16q22.2	2.58E-10	1.48E-06	87.76	6.72E-10	1.75E-06	64.41
7946977	SAA2-SAA4	SAA2-SAA4 readthrough	11p15.1	3.70E-10	1.71E-06	5.68	2.86E-10	1.05E-06	5.87
8091385	CP	ceruloplasmin (ferroxidase)	3q24q25.1	4.65E-10	1.93E-06	37.57	2.89E-10	1.05E-06	42.79
8048864	CCL20	chemokine (C-C motif) ligand 20	2q36.3	2.53E-09	8.58E-06	121.78	1.48E-09	3.04E-06	148.82
8016128	GFAP	glial fibrillary acidic protein	17q21	2.95E-09	8.80E-06	3.08	1.37E-08	1.46E-05	2.75
7904953	RNU1-120P	RNA, U1 small nuclear 120, pseudogene	1q21.2	7.32E-09	1.87E-05	15.20	3.68E-08	3.38E-05	11.01
7931108	DMBT1	deleted in malignant brain tumors 1	10q26.13	7.61E-09	1.94E-05	3.45	1.63E-09	3.17E-06	4.04
8051322	XDH	xanthine dehydrogenase	2p23.1	1.06E-08	2.37E-05	8.67	4.80E-09	7.11E-06	9.93
8164464	ZER1	zyg-11 related, cell cycle regulator	9q34.11	2.09E-08	3.69E-05	-2.88	1.21E-07	7.44E-05	-2.52
8062927	PI3	peptidase inhibitor 3, skin-derived	20q13.12	2.00E-08	3.70E-05	4.12	1.62E-07	9.20E-05	3.32
8095697	CXCL1	C-X-C motif chemokine ligand 1	4q13.3	1.90E-08	3.70E-05	11.61	5.08E-08	4.11E-05	9.68
8038556	NAPSA	napsin A aspartic peptidase	19q13.33	2.01E-08	3.72E-05	11.16	4.79E-08	3.81E-05	9.53
7946983	SAA2	serum amyloid A2	11p15.1	3.18E-08	4.87E-05	6.70	1.55E-08	1.70E-05	7.49
8103466	FSTL5	follistatin-like 5	4q32.3	6.26E-08	9.45E-05	3.91	2.63E-08	2.36E-05	4.31
7971950	DACH1	dachshund family transcription factor 1	13q22	9.45E-08	1.25E-04	3.82	8.17E-08	5.55E-05	3.87
8109039	SPINK14	serine peptidase inhibitor, Kazal type 14 (putative)	5q32	1.16E-07	1.53E-04	5.40	6.30E-08	4.71E-05	5.88
7906764	HSPA6	heat shock protein family A (Hsp70) member 6	1q23	1.39E-07	1.73E-04	20.77	1.65E-06	5.31E-04	11.79
7938758	SAA1	serum amyloid A1	11p15.1	1.80E-07	1.98E-04	7.69	1.42E-07	7.28E-05	7.95
8044976	CNTNAP5	contactin associated protein-like 5	2q14.3	2.19E-07	2.11E-04	4.93	2.24E-07	1.10E-04	4.91
7979357	OTX2	orthodenticle homeobox 2	14q22.3	2.07E-07	2.16E-04	4.66	1.28E-07	6.95E-05	4.92
7927482	CHAT	choline O-acetyltransferase	10q11.2	1.89E-07	2.18E-04	4.96	2.46E-07	1.25E-04	4.79
8135915	HILPDA	hypoxia inducible lipid droplet-associated	7q32.1	2.26E-07	2.44E-04	13.83	2.57E-07	1.28E-04	13.47
8001918	RRAD	Ras-related associated with diabetes	16q22	2.61E-07	2.69E-04	15.91	2.00E-06	6.13E-04	10.27
8056457	SCN1A	sodium channel, voltage-gated, type I, alpha subunit	2q24.3	3.02E-07	2.94E-04	3.72	2.14E-07	1.07E-04	3.87
8006459	CCL13	chemokine (C-C motif) ligand 13	17q11.2	4.10E-07	3.71E-04	8.08	3.67E-08	3.46E-05	12.69
8061916	BPIFB9P	BPI fold containing family B, member 9, pseudogene	20q11.21	6.03E-07	4.85E-04	5.56	3.31E-07	1.47E-04	6.06
8130556	SOD2	superoxide dismutase 2, mitochondrial	6q25.3	5.99E-07	5.05E-04	7.48	1.79E-06	5.72E-04	6.25
8010354	GAA	glucosidase, alpha; acid	17q25.3	8.37E-07	6.33E-04	-3.90	1.07E-06	3.78E-04	-3.81
8015387	KRT17	keratin 17	17q21.2	8.07E-07	6.39E-04	4.64	2.77E-07	1.34E-04	5.34
8075316	OSM	oncostatin M	22q12.2	8.33E-07	6.64E-04	3.43	6.68E-06	1.48E-03	2.80
8180340	RAB7B	RAB7B, member RAS oncogene family	1q32.1	1.17E-06	8.17E-04	3.13	3.62E-06	8.96E-04	2.83

8109649	MIR146A	microRNA 146a	5q34	1.39E-06	9.36E-04	3.01	8.34E-07	2.98E-04	3.19
8030860	FPR2	formyl peptide receptor 2	19q13.41	1.45E-06	9.78E-04	6.86	5.19E-06	1.24E-03	5.61
8038487	IL4I1	interleukin 4 induced 1	19q13.33	1.44E-06	9.85E-04	2.87	5.77E-06	1.28E-03	2.54
8095680	CXCL8	C-X-C motif chemokine ligand 8	4q13.3	1.58E-06	1.04E-03	39.82	8.73E-07	3.27E-04	48.30
7912145	TNFRSF9	tumor necrosis factor receptor superfamily, member 9	1p36	1.69E-06	1.08E-03	3.77	3.15E-06	8.20E-04	3.52
8070584	TMPRSS3	transmembrane protease, serine 3	21q22.3	2.13E-06	1.33E-03	5.95	3.19E-07	1.46E-04	8.04
8092970	APOD	apolipoprotein D	3q29	2.36E-06	1.44E-03	24.97	1.56E-04	1.30E-02	8.67
8043981	IL1R2	interleukin 1 receptor, type II	2q12	2.97E-06	1.79E-03	7.74	1.18E-05	2.08E-03	6.12
7905571	S100A9	S100 calcium binding protein A9	1q21	3.10E-06	1.82E-03	8.13	3.46E-05	4.64E-03	5.37
8036103	SBSN	suprabasin	19q13.13	3.13E-06	1.85E-03	3.29	3.11E-06	8.18E-04	3.29
8131803	IL6	interleukin 6	7p21	4.80E-06	2.40E-03	5.41	1.88E-05	2.91E-03	4.49
8148184	FAM83A	family with sequence similarity 83, member A	8q24.13	5.85E-06	3.00E-03	2.87	1.68E-06	5.17E-04	3.23
7967318	HCAR2	hydroxycarboxylic acid receptor 2	12q24.31	6.71E-06	3.01E-03	2.53	7.35E-06	1.32E-03	2.53
7967322	HCAR3	hydroxycarboxylic acid receptor 3	12q24.31	7.42E-06	3.30E-03	4.23	4.39E-06	9.46E-04	4.53
7930593	PLEKHS1	pleckstrin homology domain containing, family S member 1	10q25.3	9.04E-06	3.79E-03	3.33	1.20E-05	1.95E-03	3.23
7997801	IL17C	interleukin 17C	16q24	9.86E-06	4.35E-03	2.81	2.87E-05	3.95E-03	2.56
8100994	CXCL2	C-X-C motif chemokine ligand 2	4q21	8.94E-06	4.38E-03	10.63	1.01E-06	3.65E-04	17.55
8112198	ACTBL2	actin, beta-like 2	5q11.2	9.48E-06	4.54E-03	9.47	1.17E-06	4.06E-04	14.89
7906775	HSPA6	heat shock protein family A (Hsp70) member 6	1q23	9.76E-06	4.61E-03	8.61	4.66E-04	2.62E-02	4.32
8162373	OGN	osteoglycin	9q22	1.28E-05	5.61E-03	26.62	5.69E-04	3.03E-02	-9.15
7965587	RNU6-247P	RNA, U6 small nuclear 247, pseudogene	12q22q23.1	1.30E-05	5.74E-03	6.64	9.69E-06	1.85E-03	7.00
8138310	DGKB	diacylglycerol kinase, beta 90 kDa	7p21.2	1.72E-05	6.42E-03	4.50	3.44E-05	4.49E-03	4.09
8038861	SIGLEC6	sialic acid binding Ig-like lectin 6	19q13.3	1.71E-05	7.03E-03	30.33	7.96E-06	1.63E-03	38.97
8054722	IL1B	interleukin 1, beta	2q14	1.69E-05	7.10E-03	21.10	8.06E-04	3.69E-02	7.63
8096580	MTTP	microsomal triglyceride transfer protein	4q24	1.89E-05	7.44E-03	2.02	1.32E-05	2.32E-03	2.06
7900146	ZC3H12A	zinc finger CCCH-type containing 12A	1p34.3	2.52E-05	9.60E-03	3.10	6.55E-06	1.42E-03	3.58
8061912	BPIFB9P	BPI fold containing family B, member 9, pseudogene	20q11.21	3.04E-05	9.69E-03	3.43	4.25E-06	9.48E-04	4.27
8173174	USP51	ubiquitin specific peptidase 51	Xp11.21	2.59E-05	9.72E-03	-3.09	4.85E-05	6.04E-03	-2.89
7904244	MAB21L3	mab-21-like 3 (C. elegans)	1p13.1	3.55E-05	1.15E-02	3.26	1.04E-05	1.87E-03	3.77
7951217	MMP7	matrix metallopeptidase 7	11q22.2	3.81E-05	1.20E-02	18.25	2.91E-05	4.20E-03	19.70
8167887	MAGEH1	melanoma antigen family H, 1	Xp11.21	3.80E-05	1.20E-02	-4.11	4.52E-06	1.12E-03	-5.60
8104234	TRIP13	thyroid hormone receptor interactor 13	5p15.33	4.03E-05	1.31E-02	2.44	1.33E-04	1.17E-02	2.20
8046815	ZNF804A	zinc finger protein 804A	2q32.1	5.48E-05	1.35E-02	4.11	5.38E-04	2.53E-02	3.09
8147065	RALYL	RALY RNA binding protein-like	8q21.2	4.52E-05	1.39E-02	2.32	2.34E-05	3.49E-03	2.45
8156873	INVS	inversin	9q31	4.68E-05	1.42E-02	-2.40	6.27E-06	1.44E-03	-2.87
8033445	CD209	CD209 molecule	19p13	5.27E-05	1.45E-02	6.53	5.49E-05	6.13E-03	6.47
7998063	TUBB3	tubulin, beta 3 class III	16q24.3	4.80E-05	1.49E-02	2.30	1.45E-04	1.25E-02	2.11
8049075	B3GNT7	UDP-GlcNAc:betaGal beta-1,3-N-acetylglucosaminyltransferase 7	2q37.1	5.68E-05	1.50E-02	3.23	4.32E-06	1.05E-03	4.42
7955297	AQP5	aquaporin 5	12q13	5.08E-05	1.52E-02	10.24	1.26E-05	2.23E-03	14.28
7921076	GPATCH4	G patch domain containing 4	1q22	6.46E-05	1.78E-02	2.99	2.59E-05	3.75E-03	3.32
7981333	RN7SL472P	RNA, 7SL, cytoplasmic 472, pseudogene	4q32.31	6.65E-05	1.81E-02	21.88	1.62E-04	1.33E-02	16.68

7908907	ADORA1	adenosine A1 receptor	1q32.1	7.42E-05	1.94E-02	2.93	1.70E-07	9.50E-05	6.35
7923875	C1orf186	chromosome 1 open reading frame 186	1q32.1	7.92E-05	2.02E-02	5.00	1.29E-05	2.23E-03	6.78
8086961	PFKFB4	6-phosphofructo-2-kinase/fructose-2,6-biphosphatase 4	3p21.31	9.40E-05	2.26E-02	2.93	7.29E-04	3.52E-02	2.35
8155794	C9orf85	chromosome 9 open reading frame 85	9q21.13	1.40E-04	2.36E-02	-3.64	4.94E-05	5.12E-03	-4.11
7992828	IL32	interleukin 32	16p13.3	1.16E-04	2.39E-02	4.31	7.26E-04	3.20E-02	3.32
8119403	APOBEC2	apolipoprotein B mRNA editing enzyme catalytic subunit 2	6p21.1	1.57E-04	2.54E-02	3.77	1.67E-05	2.41E-03	4.95
8156581	ERCC6L2	excision repair cross-complementation group 6-like 2	9q22.32	1.20E-04	2.62E-02	-2.33	2.84E-04	1.92E-02	-2.17
8110841	LPCAT1	lysophosphatidylcholine acyltransferase 1	5p15.33	1.40E-04	2.84E-02	3.19	7.45E-05	8.10E-03	3.45
8168749	SRPX2	sushi-repeat containing protein, X-linked 2	Xq22.1	1.46E-04	2.91E-02	4.47	5.03E-06	1.22E-03	7.93
7943413	BIRC3	baculoviral IAP repeat containing 3	11q22	1.64E-04	2.97E-02	16.36	4.68E-05	5.65E-03	23.77
7909371	CR1	complement component 3b/4b receptor 1 (Knops blood group)	1q32.2	1.67E-04	3.11E-02	3.34	7.19E-04	3.38E-02	2.78
8169504	SLC6A14	solute carrier family 6 (amino acid transporter), member 14	Xq23	1.75E-04	3.13E-02	15.62	1.30E-05	2.23E-03	33.84
7983478	C15orf48	chromosome 15 open reading frame 48	15q21.1	1.71E-04	3.23E-02	6.27	1.92E-05	3.01E-03	9.84
8016033	FAM171A2	family with sequence similarity 171, member A2	17q21.31	1.93E-04	3.40E-02	-3.63	1.18E-04	1.08E-02	-3.89
8006865	PPP1R1B	protein phosphatase 1, regulatory (inhibitor) subunit 1B	17q12	2.33E-04	3.87E-02	4.06	2.91E-04	1.94E-02	3.92
8126248	UNC5CL	unc-5 homolog C (C. elegans)-like	6p21.1	2.48E-04	3.96E-02	5.01	1.87E-05	2.97E-03	8.06
8104901	IL7R	interleukin 7 receptor	5p13	2.88E-04	4.38E-02	9.07	9.49E-04	4.08E-02	6.81
7923347	LAD1	ladinin 1	1q32.1	3.19E-04	4.65E-02	3.49	5.01E-08	4.24E-05	16.03
8158725	ABL1	ABL proto-oncogene 1, non-receptor tyrosine kinase	9q34.1	3.16E-04	4.66E-02	-2.71	1.28E-04	1.17E-02	-3.01
8083233	ZIC1	Zic family member 1	3q24	6.98E-06		17.37	3.07E-02		-2.69
8072678	HMOX1	heme oxygenase (decycling) 1	22q13.1	4.33E-05		4.92	2.11E-03		2.79
8099476	PROM1	prominin 1	4p15.32	1.17E-04		16.06	1.73E-03		7.62
7988350	DUOX2	dual oxidase 2	15q15.3	1.32E-04		-19.36	4.31E-02		3.55
7953603	C1S	complement component 1, s subcomponent	12p13	1.58E-04		13.15	1.70E-02		-3.98
8122701	--	--	6q25.1	1.65E-04		-5.66	2.95E-03		-3.43
8102342	ELOVL6	ELOVL fatty acid elongase 6	4q25	1.66E-04		7.20	1.15E-02		3.09
8054712	IL1A	interleukin 1, alpha	2q14	1.68E-04		8.26	1.67E-02		3.09
8156633	CCDC180	coiled-coil domain containing 180	9q22.33	1.76E-04		-2.72	1.10E-03		-2.25
8157446	ORM1	orosomucoid 1	9q32	1.98E-04		4.95	3.07E-05		6.43
7940441	PGA3	pepsinogen 3, group I (pepsinogen A)	11q12.2	2.67E-04		3.77	9.14E-04		3.19
8157700	RABGAP1	RAB GTPase activating protein 1	9q34.11	2.85E-04		-2.84	2.51E-03		-2.23
8111220	CDH18	cadherin 18, type 2	5p14.3	3.02E-04		2.17	2.58E-04		2.22
7940177	OR4D10	olfactory receptor, family 4, subfamily D, member 10	11q12	3.19E-04		7.26	8.51E-05		9.74
8034837	DNAJB1	DnaJ (Hsp40) homolog, subfamily B, member 1	19p13.2	3.20E-04		4.41	3.91E-03		2.96
8147469	CPQ	carboxypeptidase Q	8q22.2	3.28E-04		-3.12	2.58E-04		-3.23
8094743	RHOH	ras homolog family member H	4p13	3.42E-04		3.23	1.18E-02		2.06
8156601	ERCC6L2	excision repair cross-complementation group 6-like 2	9q22.32	3.53E-04		-2.58	1.96E-03		-2.15
8130580	SNORA29	small nucleolar RNA, H/ACA box 29	6q25.3	3.69E-04		3.17	3.84E-04		3.15
8140151	RFC2	replication factor C (activator 1) 2, 40 kDa	7q11.23	3.75E-04		2.12	1.08E-05		2.91
8147461	SDC2	syndecan 2	8q22.1	3.88E-04		-2.43	1.07E-04		-2.77
8132960	SNORA22	Small nucleolar RNA SNORA22	7p11.2	3.89E-04		2.69	1.62E-03		2.30

8109677	GABRG2	gamma-aminobutyric acid (GABA) A receptor, gamma 2	5q34	4.11E-04	2.43	1.55E-04	2.67
8115584	CCNJL	cyclin J-like	5q33.3	4.53E-04	3.12	1.27E-05	5.06
8180246	--	--	--	4.73E-04	-5.54	5.84E-03	-3.53
7940431	PGA3	pepsinogen 3, group I (pepsinogen A)	11q12.2	5.30E-04	3.86	1.92E-03	3.20
8138566	IGF2BP3	insulin-like growth factor 2 mRNA binding protein 3	7p11	5.35E-04	3.34	9.50E-05	4.30
7909164	CTSE	cathepsin E	1q31	5.69E-04	92.12	2.17E-04	155.04
7952339	SNORD14C	small nucleolar RNA, C/D box 14C	11q24.1	5.93E-04	9.74	4.51E-02	3.11
8106168	--	Y_RNA ENSG00000200833	5q13.2	5.94E-04	2.51	5.69E-04	2.52
7944751	C11orf63	chromosome 11 open reading frame 63	11q24.1	6.01E-04	-3.32	6.34E-05	-4.61
7983910	AQP9	aquaporin 9	15q	6.02E-04	13.61	1.14E-03	11.19
7990818	BCL2A1	BCL2-related protein A1	15q24.3	6.13E-04	4.28	9.18E-04	4.00
7908639	C1orf106	chromosome 1 open reading frame 106	1q32.1	6.54E-04	2.49	4.25E-04	2.61
8032509	GNG7	guanine nucleotide binding protein (G protein), gamma 7	19p13.3	6.83E-04	-2.28	2.01E-07	-5.66
7940421	PGA3	pepsinogen 3, group I (pepsinogen A)	11q12.2	6.96E-04	3.67	2.50E-03	3.04
7905533	IVL	involucrin	1q21	7.00E-04	2.73	4.57E-04	2.88
8124534	HIST1H4L	histone cluster 1, H4l	6p22.1	7.22E-04	3.27	4.98E-03	2.50
7924508	SUSD4	sushi domain containing 4	1q41	7.33E-04	3.19	2.38E-05	5.16
8118310	HSPA1A	heat shock 70 kDa protein 1A	6p21.3	7.39E-04	6.05	9.50E-03	3.52
8025402	ANGPTL4	angiopoietin-like 4	19p13.3	7.58E-04	11.86	6.51E-05	25.38
8179322	HSPA1A	heat shock 70 kDa protein 1A	6p21.3	7.71E-04	6.09	9.60E-03	3.55
8123864	TFAP2A	transcription factor AP-2 alpha	6p24.3	7.76E-04	3.36	5.67E-03	2.53
8157027	NIPSNAP3B	nipsnap homolog 3B (C. elegans)	9q31.1	8.39E-04	-3.03	2.86E-03	-2.57
7951928	DSCAML1	Down syndrome cell adhesion molecule like 1	11q23	8.51E-04	2.72	5.55E-04	2.83
7907861	XPR1	xenotropic and polytropic retrovirus receptor 1	1q25.1	8.52E-04	3.02	2.79E-06	7.13
7969640	CLDN10	claudin 10	13q32.1	9.46E-04	6.07	9.87E-05	10.21
8026272	IL27RA	interleukin 27 receptor, alpha	19p13.11	1.01E-03	3.65	5.75E-04	3.99
8162388	OMD	osteomodulin	9q22.31	1.03E-03	7.74	1.55E-05	-22.52
8104449	CCT5	chaperonin containing TCP1, subunit 5 (epsilon)	5p15.2	1.04E-03	2.50	4.41E-03	2.13
7928602	SFTPA1	surfactant protein A1	10q22.3	1.05E-03	30.04	1.42E-04	71.83
7928632	SFTPA1	surfactant protein A1	10q22.3	1.05E-03	30.04	1.42E-04	71.83
8097116	RNU4-33P	RNA, U4 small nuclear 33, pseudogene	---	1.08E-03	2.44	6.65E-04	2.58
8109639	PTTG1	pituitary tumor-transforming 1	5q35.1	1.10E-03	3.70	3.55E-06	9.46
8156604	ERCC6L2	excision repair cross-complementation group 6-like 2	9q22.32	1.10E-03	-2.26	8.46E-04	-2.32
7915472	SLC2A1	solute carrier family 2 member 1	1p34.2	1.12E-03	4.81	6.13E-04	5.41
7975987	SNORA46	small nucleolar RNA, H/ACA box 46	14q24.3	1.12E-03	3.24	3.53E-03	2.75
7922756	NMNAT2	nicotinamide nucleotide adenylyltransferase 2	1q25	1.13E-03	6.39	4.52E-02	-2.72
7909681	PROX1	prospero homeobox 1	1q41	1.14E-03	4.00	1.30E-05	9.30
8124848	IER3	immediate early response 3	6p21.3	1.15E-03	4.55	2.15E-03	4.06
8179704	IER3	immediate early response 3	6p21.3	1.15E-03	4.55	2.15E-03	4.06
8106141	FCHO2	FCH domain only 2	5q13.2	1.18E-03	2.42	5.41E-05	3.44
7934698	SFTPA2	surfactant protein A2	10q22.3	1.19E-03	28.20	1.84E-04	63.22

7934708	SFTPA2	surfactant protein A2	10q22.3	1.19E-03	28.20	1.84E-04	63.22
7920244	S100A8	S100 calcium binding protein A8	1q21	1.23E-03	15.82	1.97E-02	6.11
7993638	TMC5	transmembrane channel-like 5	16p12.3	1.27E-03	3.33	2.25E-04	4.09
7996022	CCL22	chemokine (C-C motif) ligand 22	16q13	1.31E-03	2.62	9.32E-04	2.73
7977046	TNFAIP2	tumor necrosis factor, alpha-induced protein 2	14q32	1.36E-03	7.55	2.45E-03	6.49
8046408	PDK1	pyruvate dehydrogenase kinase, isozyme 1	2q31.1	1.37E-03	3.42	1.46E-03	3.38
8029465	BCL3	B-cell CLL/lymphoma 3	19q13.32	1.37E-03	3.64	3.09E-04	4.55
8157038	SLC44A1	solute carrier family 44 (choline transporter), member 1	9q31.1	1.43E-03	-3.33	1.77E-02	-2.26
7952335	SNORD14E	small nucleolar RNA, C/D box 14E	11q24.1	1.48E-03	13.41	8.05E-03	7.63
7909441	G0S2	G0/G1 switch 2	1q32.2	1.52E-03	6.18	5.85E-04	7.74
8118314	HSPA1B	heat shock 70 kDa protein 1B	6p21.3	1.54E-03	6.11	9.28E-03	4.02
8178435	IER3	immediate early response 3	6p21.3	1.63E-03	4.61	2.12E-03	4.38
8090433	MGLL	monoglyceride lipase	3q21.3	1.63E-03	4.32	8.08E-03	3.19
8156743	FOXE1	forkhead box E1 (thyroid transcription factor 2)	9q22	1.64E-03	-3.74	3.10E-04	4.98
8178086	HSPA1B	heat shock 70 kDa protein 1B	6p21.3	1.66E-03	6.10	9.98E-03	4.00
8179324	HSPA1B	heat shock 70 kDa protein 1B	6p21.3	1.66E-03	6.10	9.98E-03	4.00
8114249	CXCL14	chemokine (C-X-C motif) ligand 14	5q31	1.67E-03	52.97	3.70E-04	117.45
8098637	CYP4V2	cytochrome P450, family 4, subfamily V, polypeptide 2	4q35.2	1.75E-03	-2.67	5.51E-03	-2.29
7988426	SLC30A4	solute carrier family 30 (zinc transporter), member 4	15q21.1	1.81E-03	-2.66	8.77E-04	-2.92
8075886	IL2RB	interleukin 2 receptor, beta	22q13.1	1.82E-03	3.91	3.74E-03	3.46
8140504	MAGI2	membrane associated guanylate kinase, WW and PDZ domain containing 2	7q21.11	1.83E-03	-3.01	1.27E-04	-4.51
8065344	FOXA2	forkhead box A2	20p11	1.88E-03	2.55	7.04E-04	2.89
7937079	BNIP3	BCL2/adenovirus E1B 19 kDa interacting protein 3	–	1.91E-03	2.74	4.12E-06	6.68
7976698	EML1	echinoderm microtubule associated protein like 1	14q32	1.93E-03	-4.17	2.49E-03	-3.97
8103894	ENPP6	ectonucleotide pyrophosphatase/phosphodiesterase 6	4q35.1	1.95E-03	3.04	3.67E-09	-43.97
8126820	GPR110	G protein-coupled receptor 110	6p12.3	2.23E-03	6.42	1.30E-06	54.13
8080847	C3orf14	chromosome 3 open reading frame 14	3p14.2	2.29E-03	-3.02	2.50E-04	-4.11
8037374	PLAUR	plasminogen activator, urokinase receptor	19q13	2.32E-03	3.87	1.47E-02	2.77
7923850	SLC26A9	solute carrier family 26 (anion exchanger), member 9	1q32.1	2.35E-03	12.40	3.87E-04	23.32
8139433	MYO1G	myosin IG	7p13	2.49E-03	25.19	5.86E-04	48.18
8167027	RGN	regucalcin	Xp11.3	2.60E-03	-2.89	3.72E-04	3.77
8155930	GCNT1	glucosaminyl (N-acetyl) transferase 1, core 2	9q13	2.62E-03	-4.66	3.14E-02	2.73
7925589	SMYD3	SET and MYND domain containing 3	1q44	2.63E-03	3.81	6.28E-05	7.63
8130645	PARK2	parkin RBR E3 ubiquitin protein ligase	6q26	2.70E-03	-2.34	1.17E-04	-3.43
7918533	ADORA3	adenosine A3 receptor	1p13.2	2.72E-03	3.75	4.21E-02	-2.26
8104307	C5orf38	chromosome 5 open reading frame 38	5p15.33	2.91E-03	5.03	2.92E-03	5.03
8106923	NR2F1	nuclear receptor subfamily 2, group F, member 1	5q14	2.97E-03	2.88	1.69E-03	-3.13
8162059	SLC28A3	solute carrier family 28 (concentrative nucleoside transport	9q21.32q21.33	3.08E-03	3.68	3.12E-04	5.55
8163795	PSMD5	proteasome (prosome, macropain) 26S subunit, non-ATPase, 5	9q33.2	3.12E-03	-3.66	1.65E-03	-4.11
7930921	BAG3	BCL2-associated athanogene 3	10q26.11	3.33E-03	2.39	8.90E-04	2.81
8087739	CISH	cytokine inducible SH2-containing protein	3p21.3	3.49E-03	2.50	1.62E-06	7.76

7933084	NAMPT	nicotinamide phosphoribosyltransferase	7q22.3	3.59E-03	4.88	2.50E-02	3.12
8144488	LINC00965	long intergenic non-protein coding RNA 965	8p23.1	3.62E-03	-2.72	2.41E-03	-2.88
8070467	TMPRSS2	transmembrane protease, serine 2	21q22.3	3.63E-03	10.95	1.60E-04	33.23
8065607	PLAGL2	pleiomorphic adenoma gene-like 2	20q11.21	3.65E-03	2.24	7.92E-04	2.67
8142120	NAMPT	nicotinamide phosphoribosyltransferase	7q22.3	3.74E-03	4.79	3.48E-02	2.87
8161418	--	--	--	3.81E-03	3.53	1.41E-04	6.54
8051133	FTH1P3	ferritin, heavy polypeptide 1 pseudogene 3	2p23.3	3.95E-03	2.46	5.43E-03	2.36
8062395	NNAT	neuronatin	20q11.23	3.97E-03	60.79	1.81E-02	24.33
8064939	TMX4	thioredoxin-related transmembrane protein 4	20p12	4.10E-03	-2.96	1.52E-02	-2.41
8009443	ARSG	arylsulfatase G	17q24.2	4.27E-03	-2.47	3.22E-03	-2.57
7912638	TMEM51-AS1	TMEM51 antisense RNA 1	1p36.21	4.33E-03	2.42	6.91E-03	2.28
8099834	TLR1	toll-like receptor 1	4p14	4.59E-03	2.74	3.67E-03	-2.80
7968212	WASF3	WAS protein family, member 3	13q12	4.62E-03	-3.40	1.10E-04	-6.85
8120552	FAM135A	family with sequence similarity 135, member A	6q13	4.70E-03	-2.54	7.31E-04	-3.30
8144410	LINC00965	long intergenic non-protein coding RNA 965	8p23.1	4.72E-03	-3.50	5.77E-03	-3.37
7940175	OR4D6	olfactory receptor, family 4, subfamily D, member 6	11q12.1	4.76E-03	5.40	1.48E-03	7.22
7908924	PRELP	proline/arginine-rich end leucine-rich repeat protein	1q32.1	4.84E-03	4.24	4.23E-03	-4.33
7919028	TBX15	T-box 15	1p11.1	4.86E-03	3.25	2.91E-05	-8.42
7978544	EGLN3	egl-9 family hypoxia-inducible factor 3	14q13.1	4.92E-03	3.77	1.08E-02	3.25
8086185	PLCD1	phospholipase C, delta 1	3p22.2	4.92E-03	-2.73	1.39E-03	-3.31
7953735	LINC00965	long intergenic non-protein coding RNA 965	8p23.1	5.11E-03	-3.16	7.00E-03	-2.99
8032834	LRG1	leucine-rich alpha-2-glycoprotein 1	19p13.3	5.11E-03	2.30	8.89E-04	2.78
7938777	LDHA	lactate dehydrogenase A	11p15.4	5.11E-03	3.14	3.87E-02	2.20
8043441	IGKV1D-27	immunoglobulin kappa variable 1D-27 (pseudogene)	2p11.2	5.14E-03	4.29	6.82E-03	4.05
7907171	BLZF1	basic leucine zipper nuclear factor 1	1q24	5.22E-03	2.13	2.30E-03	2.34
7903959	PIFO	primary cilia formation	1p13.2	5.36E-03	-2.72	1.99E-02	2.23
7922976	PTGS2	prostaglandin-endoperoxide synthase 2	1q31.1	5.41E-03	10.38	1.24E-03	17.62
8025601	ICAM1	intercellular adhesion molecule 1	19p13.2	5.48E-03	5.44	2.60E-04	12.12
8116983	CD83	CD83 molecule	6p23	5.52E-03	3.03	1.76E-03	3.66
8025382	CERS4	ceramide synthase 4	19p13.2	5.73E-03	-2.38	1.09E-02	2.18
8006433	CCL2	chemokine (C-C motif) ligand 2	17qq12	5.86E-03	12.01	1.38E-02	8.64
7937852	SLC22A18	solute carrier family 22, member 18	11p15.5	5.87E-03	2.10	2.47E-03	2.32
8162610	CDC14B	cell division cycle 14B	9q22.3	5.94E-03	-3.16	7.52E-03	-3.03
7922243	METTL18	methyltransferase like 18	1q24.2	6.04E-03	3.21	6.56E-04	4.81
7931930	PRKCQ	protein kinase C, theta	10p15	6.07E-03	-2.21	5.40E-05	4.06
7931914	IL2RA	interleukin 2 receptor, alpha	10p15.1	6.08E-03	4.26	2.50E-02	3.09
7967544	SCARB1	scavenger receptor class B, member 1	12q24.31	6.24E-03	-2.50	8.25E-04	-3.35
7984588	THSD4	thrombospondin, type I, domain containing 4	15q23	6.28E-03	-2.39	9.22E-09	-25.45
8054580	BUB1	BUB1 mitotic checkpoint serine/threonine kinase	2q13	6.34E-03	4.47	5.12E-04	8.13
8006594	CCL18	C-C motif chemokine ligand 18	17q12	6.43E-03	14.96	1.92E-04	68.79
8144416	LINC00965	long intergenic non-protein coding RNA 965	8p23.1	6.48E-03	-3.60	8.52E-03	-3.40

8144418	LINC00965	long intergenic non-protein coding RNA 965	8p23.1	6.48E-03	-3.60	8.52E-03	-3.40
8144490	LINC00965	long intergenic non-protein coding RNA 965	8p23.1	6.48E-03	-3.60	8.52E-03	-3.40
8144492	LINC00965	long intergenic non-protein coding RNA 965	8p23.1	6.48E-03	-3.60	8.52E-03	-3.40
8148501	PTP4A3	protein tyrosine phosphatase type IVA, member 3	8q24.3	6.59E-03	4.15	2.38E-04	8.82
7909214	RASSF5	Ras association domain family member 5	1q32.1	6.66E-03	3.05	3.26E-03	3.45
7946401	ST5	suppression of tumorigenicity 5	11p15	6.68E-03	2.76	9.50E-03	2.62
8098423	NEIL3	nei endonuclease VIII-like 3 (E. coli)	4q34.3	6.93E-03	2.83	3.99E-03	3.10
8042144	REL	v-rel avian reticuloendotheliosis viral oncogene homolog	2p13	6.96E-03	2.99	1.12E-03	4.12
8111772	DAB2	Dab, mitogen-responsive phosphoprotein, homolog 2 (Drosophila)	5p13.1	7.05E-03	3.89	3.54E-02	-2.73
8149218	LINC00965	long intergenic non-protein coding RNA 965	8p23.1	7.11E-03	-3.59	9.38E-03	-3.39
8149220	LINC00965	long intergenic non-protein coding RNA 965	8p23.1	7.11E-03	-3.59	9.38E-03	-3.39
8149222	LINC00965	long intergenic non-protein coding RNA 965	8p23.1	7.11E-03	-3.59	9.38E-03	-3.39
8149224	LINC00965	long intergenic non-protein coding RNA 965	8p23.1	7.11E-03	-3.59	9.38E-03	-3.39
8149226	LINC00965	long intergenic non-protein coding RNA 965	8p23.1	7.11E-03	-3.59	9.38E-03	-3.39
8157300	BSPRY	B-box and SPRY domain containing	9q32	7.20E-03	-2.28	9.58E-04	2.98
8141076	PON2	paraoxonase 2	7q21.3	7.29E-03	2.62	1.30E-02	2.41
8099541	QDPR	quinoid dihydropteridine reductase	4p15.31	7.30E-03	-3.34	1.33E-02	-3.00
8149161	LINC00965	long intergenic non-protein coding RNA 965	8p23.1	7.31E-03	-3.30	7.36E-03	-3.29
8149210	LINC00965	long intergenic non-protein coding RNA 965	8p23.1	7.31E-03	-3.30	7.36E-03	-3.29
8149228	LINC00965	long intergenic non-protein coding RNA 965	8p23.1	7.37E-03	-3.14	1.11E-02	-2.92
8088979	VGLL3	vestigial-like family member 3	3p12.1	7.51E-03	2.31	3.71E-03	2.55
8043697	ANKRD36B	ankyrin repeat domain 36B	2q11.2	7.52E-03	-3.05	2.11E-02	-2.56
8161964	FRMD3	FERM domain containing 3	9q21.32	7.57E-03	-3.99	3.35E-03	4.87
8167728	SSX2B	synovial sarcoma, X breakpoint 2B	Xp11.22	7.64E-03	2.75	5.52E-05	6.04
8149216	LINC00965	long intergenic non-protein coding RNA 965	8p23.1	7.76E-03	-3.48	1.01E-02	-3.29
8144420	LINC00965	long intergenic non-protein coding RNA 965	8p23.1	7.78E-03	-3.38	7.03E-03	-3.45
8144494	LINC00965	long intergenic non-protein coding RNA 965	8p23.1	7.78E-03	-3.38	7.03E-03	-3.45
8149151	LINC00965	long intergenic non-protein coding RNA 965	8p23.1	7.80E-03	-3.35	8.85E-03	-3.26
8149214	LINC00965	long intergenic non-protein coding RNA 965	8p23.1	7.80E-03	-3.35	8.85E-03	-3.26
8149153	LINC00965	long intergenic non-protein coding RNA 965	8p23.1	7.88E-03	-3.34	7.65E-03	-3.35
8149157	LINC00965	long intergenic non-protein coding RNA 965	8p23.1	7.88E-03	-3.34	7.65E-03	-3.35
8144412	LINC00965	long intergenic non-protein coding RNA 965	8p23.1	7.88E-03	-3.20	1.04E-02	-3.04
8144414	LINC00965	long intergenic non-protein coding RNA 965	8p23.1	7.88E-03	-3.20	1.04E-02	-3.04
7948229	SLC43A3	solute carrier family 43, member 3	11q11	7.88E-03	6.63	6.48E-03	7.05
8095819	FAM47E	family with sequence similarity 47, member E	4q21.1	7.88E-03	-2.67	1.27E-03	3.55
7980485	DIO2	deiodinase, iodothyronine, type II	14q31.1	8.03E-03	-4.83	2.82E-02	3.48
7934297	--	Y_RNA ENSG00000201047	10q22.1	8.36E-03	3.82	2.14E-02	3.17
8149165	LINC00965	long intergenic non-protein coding RNA 965	8p23.1	8.48E-03	-3.39	9.75E-03	-3.30
8149167	LINC00965	long intergenic non-protein coding RNA 965	8p23.1	8.48E-03	-3.39	9.75E-03	-3.30
7918064	COL11A1	collagen, type XI, alpha 1	1p21	8.50E-03	2.58	8.06E-05	-5.38
8103520	TRIM61	tripartite motif containing 61	4q32.3	8.50E-03	-2.86	7.51E-03	-2.92

7986509	DNM1P46	dynamin 1 pseudogene 46	15q26.3	8.59E-03	-4.86	3.81E-03	-6.00
7986512	DNM1P46	dynamin 1 pseudogene 46	15q26.3	8.59E-03	-4.86	3.81E-03	-6.00
7986527	DNM1P46	dynamin 1 pseudogene 46	15q26.3	8.59E-03	-4.86	3.81E-03	-6.00
8105436	MAP3K1	mitogen-activated protein kinase kinase kinase 1	5q11.2	8.62E-03	2.07	4.76E-07	8.08
8054439	ST6GAL2	ST6 beta-galactosamide alpha-2,6-sialyltranferase 2	2q11.3	8.72E-03	-2.94	6.26E-06	11.93
8124574	ZSCAN12	zinc finger and SCAN domain containing 12	6p21	8.72E-03	-2.41	1.81E-03	-2.99
7927186	RASSF4	Ras association domain family member 4	10q11.21	8.78E-03	3.47	1.21E-03	5.23
8124654	GABBR1	gamma-aminobutyric acid (GABA) B receptor, 1	6p21.31	8.85E-03	-2.98	1.41E-03	-4.14
8164521	SH3GLB2	SH3-domain GRB2-like endophilin B2	9q34	8.91E-03	-2.51	2.90E-03	-2.97
7953981	ETV6	ets variant 6	12p13	8.92E-03	2.33	7.75E-04	3.27
7945663	IFITM10	interferon induced transmembrane protein 10	11p15.5	8.92E-03	3.39	2.23E-02	2.82
8148304	TRIB1	tribbles pseudokinase 1	8q24.13	9.07E-03	-2.32	1.24E-04	4.30
8040223	RRM2	ribonucleotide reductase M2	2p25.1	9.41E-03	3.26	1.33E-03	4.74
8053467	SFTPB	surfactant protein B	2p11.2	9.50E-03	35.26	7.31E-04	164.67
7976816	SNORD114-3	small nucleolar RNA, C/D box 114-3	14q32.31	9.55E-03	6.30	7.29E-03	-6.85
8179595	GABBR1	gamma-aminobutyric acid (GABA) B receptor, 1	6p21.31	9.67E-03	-3.36	2.08E-03	-4.57
8117572	ZNF391	zinc finger protein 391	6p22.1	9.84E-03	-2.51	3.64E-03	-2.92
7981718	EPC1	enhancer of polycomb homolog 1 (Drosophila)	10p11	1.02E-02	10.02	2.70E-02	6.84
7919168	PDE4DIP	phosphodiesterase 4D interacting protein	1q12	1.02E-02	2.65	1.73E-02	2.43
8143850	CDK5	cyclin-dependent kinase 5	7q36	1.02E-02	2.98	2.49E-03	3.87
8155696	FAM122A	family with sequence similarity 122A	9q21.11	1.04E-02	-2.25	2.48E-04	-3.78
8119161	PIM1	Pim-1 proto-oncogene, serine/threonine kinase	6p21.2	1.04E-02	2.44	1.26E-02	2.37
7981046	IFI27L2	interferon, alpha-inducible protein 27-like 2	14q32.12	1.05E-02	-2.12	2.50E-03	-2.55
8178298	GABBR1	gamma-aminobutyric acid (GABA) B receptor, 1	6p21.31	1.05E-02	-3.24	1.63E-03	-4.69
8166264	--	--		1.05E-02	2.25	1.32E-02	2.19
7902913	CDC7	cell division cycle 7	1p22	1.06E-02	2.97	1.95E-03	4.05
8062427	VSTM2L	V-set and transmembrane domain containing 2 like	20q11.23	1.06E-02	2.55	3.36E-03	3.05
8022803	GAREM	GRB2 associated, regulator of MAPK1	18q12.1	1.07E-02	3.20	1.58E-02	2.99
7929282	HHEX	hematopoietically expressed homeobox	10q23.33	1.07E-02	-3.39	3.08E-02	2.71
8098328	GALNT7	polypeptide N-acetylgalactosaminyltransferase 7	4q31.1	1.08E-02	-2.02	7.96E-06	5.16
8094190	CC2D2A	coiled-coil and C2 domain containing 2A	4p15.32	1.08E-02	-2.82	3.04E-03	-3.51
7996160	LOC388282	uncharacterized LOC388282	16q13	1.09E-02	2.71	1.55E-03	3.72
8093171	MFI2	MFI2 antisense RNA 1	3q29	1.09E-02	3.48	9.59E-04	5.88
8157463	C9orf91	chromosome 9 open reading frame 91	9q32	1.13E-02	-2.31	1.31E-03	-3.11
8123951	ADTRP	androgen-dependent TFPI-regulating protein	6p24.1	1.13E-02	5.42	1.25E-04	20.81
8160033	SNRPE	small nuclear ribonucleoprotein polypeptide E	1q32	1.15E-02	2.26	1.46E-02	2.19
8022506	RNU6-702P	RNA, U6 small nuclear 702, pseudogene	--	1.17E-02	2.26	1.40E-02	2.21
8043360	IGKV3OR2-268	immunoglobulin kappa variable 3/OR2-268 (non-functional)	2p11.2	1.18E-02	2.94	9.03E-03	3.09
8158406	TBC1D13	TBC1 domain family, member 13	9q34.11	1.19E-02	-2.26	3.59E-03	-2.68
7986520	LOC101927628	uncharacterized LOC101927628	15q26.3	1.21E-02	-4.78	6.05E-03	-5.78
8104825	BRIX1	BRX1, biogenesis of ribosomes, homolog (S. cerevisiae)	5p13.2	1.22E-02	2.22	1.37E-02	2.18

8053801	ANKRD36	ankyrin repeat domain 36	2q11.2	1.25E-02	-2.38	1.06E-02	-2.46
7973743	BNIP3P1	BCL2/adenovirus E1B 19 kDa interacting protein 3 pseudogene 1	14q12	1.27E-02	2.59	3.98E-04	4.51
8081548	PVRL3	poliovirus receptor-related 3	3q13	1.29E-02	-4.93	3.52E-02	-3.69
7986517	DNM1P47	dynamin 1 pseudogene 47	15q26.3	1.31E-02	-4.80	6.20E-03	-5.91
7986522	DNM1P47	dynamin 1 pseudogene 47	15q26.3	1.31E-02	-4.80	6.20E-03	-5.91
8001449	IRX3	iroquois homeobox 3	16q12.2	1.36E-02	4.29	2.60E-02	3.62
7960177	SLC6A12	solute carrier family 6 member 12	12p13.33	1.40E-02	2.89	1.91E-04	6.40
7909127	MFSD4	major facilitator superfamily domain containing 4	1q32.1	1.40E-02	2.17	2.43E-03	2.77
8150988	ASPH	aspartate beta-hydroxylase	8q12.1	1.41E-02	-2.03	4.75E-03	-2.33
8159501	LCN12	lipocalin 12	9q34.3	1.41E-02	-2.76	1.43E-02	2.75
8163444	ZFP37	ZFP37 zinc finger protein	9q32	1.43E-02	-3.23	1.32E-02	-3.28
7943376	KIAA1377	KIAA1377	11q22.1	1.43E-02	-3.17	1.15E-02	-3.31
8009417	KPNA2	karyopherin alpha 2 (RAG cohort 1, importin alpha 1)	17q24.2	1.44E-02	2.35	2.19E-02	2.21
8019737	KPNA2	karyopherin alpha 2 (RAG cohort 1, importin alpha 1)	17q24.2	1.51E-02	2.32	2.14E-02	2.20
8170630	PNMA6A	paraneoplastic Ma antigen family member 6A	Xq28	1.51E-02	-2.35	5.94E-03	-2.72
8172787	SSX2B	synovial sarcoma, X breakpoint 2B	Xp11.22	1.53E-02	2.76	7.52E-05	6.84
7920264	S100A5	S100 calcium binding protein A5	1q21	1.56E-02	3.10	7.21E-04	5.85
8043470	IGKV3D-11	immunoglobulin kappa variable 3D-11	2p11.2	1.57E-02	6.36	1.91E-02	5.95
8140840	STEAP4	STEAP family member 4	7q21.12	1.59E-02	10.09	1.62E-02	10.02
8059852	MSL3P1	male-specific lethal 3 homolog (Drosophila) pseudogene 1	2q37	1.60E-02	-3.20	7.53E-03	-3.75
8138527	STEAP1B	STEAP family member 1B	7p15.3	1.65E-02	2.32	2.87E-03	3.01
8038126	CA11	carbonic anhydrase XI	19q13.3	1.68E-02	-3.52	4.21E-02	-2.82
8021169	LIPG	lipase, endothelial	18q21.1	1.69E-02	-3.83	2.51E-04	11.09
8068383	CLIC6	chloride intracellular channel 6	21q22.12	1.70E-02	-4.84	4.62E-03	-7.10
8174937	TENM1	teneurin transmembrane protein 1	Xq25	1.71E-02	-6.94	4.14E-02	5.00
7996027	CX3CL1	chemokine (C-X3-C motif) ligand 1	16q13	1.72E-02	3.54	9.46E-03	4.07
8043449	IGKV3D-20	immunoglobulin kappa variable 3D-20	2p11.2	1.74E-02	5.18	2.03E-02	4.93
7910398	RAB4A	RAB4A, member RAS oncogene family	1q42.13	1.75E-02	2.40	2.11E-02	2.33
8145281	SLC25A37	solute carrier family 25 member 37	8p21.2	1.76E-02	2.59	4.30E-03	3.32
7919971	RFX5	regulatory factor X, 5 (influences HLA class II expression)	1q21.3	1.78E-02	2.17	1.92E-02	2.15
8146839	C8orf34	chromosome 8 open reading frame 34	8q13	1.79E-02	4.29	4.52E-03	-6.40
8131583	BZW2	basic leucine zipper and W2 domains 2	7p21.1	1.80E-02	2.32	2.88E-04	4.42
7940182	OR4D10	olfactory receptor, family 4, subfamily D, member 10	11q12	1.82E-02	3.68	5.05E-03	5.04
7943803	DIXDC1	DIX domain containing 1	11q23.1	1.82E-02	-2.55	1.37E-03	-4.03
7960865	SLC2A3	solute carrier family 2 member 3	12p13.31	1.83E-02	4.96	7.78E-03	6.41
7986515	DNM1P47	dynamin 1 pseudogene 47	15q26.3	1.83E-02	-4.27	1.04E-02	-4.99
7986525	DNM1P47	dynamin 1 pseudogene 47	15q26.3	1.83E-02	-4.27	1.04E-02	-4.99
8133976	DBF4	DBF4 zinc finger	7q21.3	1.90E-02	2.23	8.51E-03	2.52
8102247	RPL34-AS1	RPL34 antisense RNA 1 (head to head)	4q25	1.91E-02	-2.49	1.44E-02	-2.63
8108301	KIF20A	kinesin family member 20A	5q31	1.92E-02	3.97	1.08E-02	4.63
8131944	NFE2L3	nuclear factor, erythroid 2-like 3	7p15.2	1.92E-02	4.67	3.64E-03	7.51

7908793	ELF3	E74 like ETS transcription factor 3	1q32.1	1.93E-02	4.56	1.40E-04	19.55
8107706	LMNB1	lamin B1	5q23.2	1.93E-02	2.02	7.06E-04	3.17
8056184	ITGB6	integrin, beta 6	2q24.2	1.95E-02	7.26	3.44E-05	88.60
8161520	PGM5	phosphoglucomutase 5	9q13	1.99E-02	-2.07	5.79E-08	-17.86
7905406	CGN	cingulin	1q21	2.03E-02	2.37	4.25E-05	6.64
7923189	KIF14	kinesin family member 14	1q32.1	2.04E-02	2.55	7.59E-03	3.05
7980098	ALDH6A1	aldehyde dehydrogenase 6 family, member A1	14q24.3	2.04E-02	-2.36	2.34E-03	-3.38
8115666	NUDCD2	NudC domain containing 2	5q34	2.06E-02	2.21	1.65E-02	2.28
8097017	UGT8	UDP glycosyltransferase 8	4q26	2.07E-02	3.33	4.47E-04	7.87
7981722	IGHV3-7	immunoglobulin heavy variable 3-7	14q32.33	2.08E-02	9.22	4.35E-02	6.64
8040458	KCNS3	potassium voltage-gated channel modifier subfamily S member 3	2p24.2	2.09E-02	2.86	4.77E-04	6.07
8109612	ADRA1B	adrenoceptor alpha 1B	5q33.3	2.09E-02	2.68	6.36E-03	3.36
8077899	PPARG	peroxisome proliferator-activated receptor gamma	3p25	2.11E-02	2.86	1.13E-02	3.25
8154670	IFT74	intraflagellar transport 74	9p21.2	2.12E-02	-2.55	2.49E-02	-2.47
8025478	ZNF559	zinc finger protein 559	19p13.2	2.14E-02	-2.44	1.16E-02	-2.71
8068833	PDE9A	phosphodiesterase 9A	21q22.3	2.15E-02	2.34	1.44E-05	8.32
8143663	EZH2	enhancer of zeste 2 polycomb repressive complex 2 subunit	7q36.1	2.23E-02	2.77	3.40E-03	4.04
7990151	PKM	pyruvate kinase, muscle	15q22	2.25E-02	2.26	3.91E-02	2.06
8145570	ESCO2	establishment of sister chromatid cohesion N-acetyltransferase 2	8p21.1	2.26E-02	3.23	7.28E-03	4.18
8161945	RASEF	RAS and EF-hand domain containing	9q21.32	2.28E-02	-2.39	1.69E-04	5.75
8021470	PMAIP1	phorbol-12-myristate-13-acetate-induced protein 1	18q21.32	2.28E-02	6.57	5.85E-03	10.91
8169235	FRMPD3	FERM and PDZ domain containing 3	Xq22	2.28E-02	3.30	1.65E-03	6.11
8167835	TRO	trophinin	Xp11.21	2.30E-02	-2.44	1.36E-03	-3.96
8110478	ZNF454	zinc finger protein 454	5q35.3	2.33E-02	-2.56	4.51E-03	-3.44
8037322	ETHE1	ethylmalonic encephalopathy 1	19q13.31	2.37E-02	2.37	2.19E-02	2.40
8063923	SLCO4A1	solute carrier organic anion transporter family, member 4A1	20q13.33	2.38E-02	2.35	2.25E-03	3.47
7988380	DUOXA1	dual oxidase maturation factor 1	15q21.1	2.39E-02	-2.80	3.58E-02	2.57
8147030	STMN2	stathmin 2	8q21.13	2.46E-02	4.01	9.76E-03	5.20
7910001	DEGS1	delta(4)-desaturase, sphingolipid 1	1q42.11	2.47E-02	2.20	5.45E-03	2.80
8083166	TRPC1	transient receptor potential cation channel subfamily C member 1	3q23	2.49E-02	-2.87	3.40E-04	-7.07
8126303	TREM1	triggering receptor expressed on myeloid cells 1	6p21.1	2.53E-02	5.91	1.73E-03	15.39
8056363	SLC38A11	solute carrier family 38, member 11	2q24.3	2.55E-02	3.06	9.82E-03	3.80
8040365	TRIB2	tribbles pseudokinase 2	2p24.3	2.59E-02	2.43	2.35E-02	-2.49
8123936	NEDD9	neural precursor cell expressed, developmentally down-regulated 9	6p24.2	2.60E-02	3.74	1.21E-02	4.60
8144228	FLJ36840	uncharacterized LOC645524	–	2.69E-02	-2.45	2.40E-02	-2.51
8044499	SLC20A1	solute carrier family 20 (phosphate transporter), member 1	2q14.1	2.94E-02	2.80	1.14E-03	5.38
8112376	CENPK	centromere protein K	5q12.3	3.01E-02	2.50	7.95E-04	5.02
8065719	PXMP4	peroxisomal membrane protein 4, 24 kDa	20q11.22	3.03E-02	-5.07	1.78E-02	-6.09
8084206	B3GNT5	UDP-GlcNAc:betaGal beta-1,3-N-acetylglucosaminyltransferase 5	3q27.1	3.08E-02	2.63	1.52E-02	3.05
8043476	IGKV1D-43	immunoglobulin kappa variable 1D-43	2p11.2	3.11E-02	3.43	4.03E-02	3.20
7909601	SNORA16B	small nucleolar RNA, H/ACA box 16B	1q32.3	3.15E-02	2.79	1.15E-02	3.48

7940173	OR5A1	olfactory receptor, family 5, subfamily A, member 1	11q12.1	3.25E-02	2.36	8.99E-03	2.96
7915910	PDZK1IP1	PDZK1 interacting protein 1	1p33	3.25E-02	8.78	7.85E-03	16.83
7953218	RAD51AP1	RAD51 associated protein 1	12p13.32	3.26E-02	2.07	1.71E-03	3.26
8054281	LONRF2	LON peptidase N-terminal domain and ring finger 2	2q11.2	3.32E-02	-2.47	1.89E-02	2.77
8001104	IGHV3OR16-7	immunoglobulin heavy variable 3/OR16-7 (pseudogene)	16p11.2	3.46E-02	4.66	4.02E-02	4.42
7906930	NUF2	NUF2, NDC80 kinetochore complex component	1q23.3	3.46E-02	2.83	1.07E-02	3.70
8124402	HIST1H1T	histone cluster 1, H1t	6p21.3	3.47E-02	2.13	1.06E-02	2.59
7917503	GBP3	guanylate binding protein 3	1p22.2	3.52E-02	3.52	5.11E-03	5.96
8007071	CDC6	cell division cycle 6	17q21.3	3.52E-02	2.21	2.13E-03	3.59
8103822	VEGFC	vascular endothelial growth factor C	4q34.3	3.61E-02	-2.20	7.95E-04	4.25
7990054	UACA	uveal autoantigen with coiled-coil domains and ankyrin repeats	15q23	3.66E-02	-3.02	3.65E-02	-3.02
8165735	CSF2RA	colony stimulating factor 2 receptor alpha subunit	Xp22.33	3.76E-02	2.37	2.82E-02	-2.51
8176306	CSF2RA	colony stimulating factor 2 receptor alpha subunit	Xp22.33	3.76E-02	2.37	2.82E-02	-2.51
8096845	EGF	epidermal growth factor	4q25	3.77E-02	2.43	9.81E-04	4.97
8115397	FAXDC2	fatty acid hydroxylase domain containing 2	5q33.2	3.80E-02	-3.10	3.54E-03	-5.63
7907830	QSOX1	quiescin Q6 sulfhydryl oxidase 1	1q24	3.85E-02	2.56	1.37E-02	3.19
7927710	CDK1	cyclin-dependent kinase 1	10q21.1	3.89E-02	3.32	1.03E-02	4.75
8019857	NDC80	NDC80 kinetochore complex component	18p11.32	3.90E-02	2.09	5.86E-03	2.85
8169598	ZCCHC12	zinc finger, CCHC domain containing 12	Xq24	3.90E-02	-3.17	5.98E-06	35.85
8146500	LYN	LYN proto-oncogene, Src family tyrosine kinase	8q13	3.98E-02	3.12	1.57E-02	3.98
7979505	SIX1	SIX homeobox 1	14q23.1	4.05E-02	2.87	3.74E-05	-15.94
7905731	UBAP2L	ubiquitin associated protein 2-like	1q21.3	4.11E-02	2.13	2.60E-02	2.30
7905929	EFNA1	ephrin-A1	1q21.3q22	4.21E-02	2.54	2.99E-03	4.44
8115623	ATP10B	ATPase, class V, type 10B	5q34	4.55E-02	2.91	3.24E-03	5.59
7932132	FRMD4A	FERM domain containing 4A	10p13	4.64E-02	2.32	4.60E-02	-2.32